scientific reports

Check for updates

OPEN

Single cell profiling of ER stress in coronary artery disease and therapeutic mechanisms of Ginkgo biloba extract

Feng-jin Zhao[2,5,6]✉, Feng Wang[3], Cheng Qin[4,6]✉ & Li-li Ye[1,2,6]✉

Coronary artery disease (CAD) is a primarily inflammatory condition caused by atherosclerosis in the coronary arteries. Increasing evidence suggests that endoplasmic reticulum (ER) stress is closely involved in the development of CAD. In the arteries of CAD patients, the degree of ER stress may increase due to endothelial cell damage and the presence of inflammatory reactions. The aim of this study was to identify ERS-related genes (ERSRGs) and potential drugs for treating CAD. Gene expression data for CAD patients and healthy controls were retrieved from the GEO database, while the ERs-related gene set was sourced from GeneCards for analysis. Differentially expressed genes (DEGs) between CAD and control groups were identified, followed by GO, KEGG, GSEA, and GSVA analyses to explore differences. WGCNA and differential expression analysis were applied to identify key modules and genes associated with CAD, and the CIBERSORT algorithm was used to assess immune cell infiltration. Nomogram is used for gene risk scoring in CAD. Additionally, a TF-miRNA-mRNA network was built to explore the regulatory mechanisms of central genes and identify upstream regulators. The DGIdb database was used to identify potential therapeutic drugs or compounds targeting these central genes. The drug predicted to be most closely associated with ERSRGs using the BATMAN-TCM database is Ginkgo biloba extract(GBE), and the strong effect of GBE in regulating ER stress was verified in cell experiments. Single-cell RNA sequencing analysis of ERSRGs was also conducted. In this study, 833 DEGs and 10 ERSRGs were identified from CAD patients and healthy controls, which showed good diagnostic value and high correlation. Functional enrichment and immune infiltration analyses revealed notable differences in gene expression, biological functions, and enriched pathways between CAD patients and healthy individuals. Drug prediction analysis identified 177 potential therapeutic drugs for CAD, especially GBE, and verified the strong effect of GBE in regulating ER stress in cell experiments. Finally, real-time quantitative PCR of human peripheral blood validated our findings. In single-cell RNA sequencing analysis, the cell source specificity of ERSRGs in transcriptome changes has been validated, providing a cellular context basis for its functional mechanism in CAD. The results indicate that ER stress plays an important role in the pathogenesis of CAD, and several promising feature genes were identified, forming a genetic risk score model for CAD, while a strong effect of GBE in the regulation of ER stress has been detected.This study provides a new comprehensive perspective on the pathways and interaction networks of ERSRGs, and lays the foundation for future personalized diagnosis and treatment.

Keywords Coronary artery disease, Endoplasmic reticulum stress, Immune infiltration, TF-miRNA-mRNA, Single cell profiling, Ginkgo biloba extract

[1]Department of Cardiovascular Medicine, GuangDong Engineering Technology Research Center of Biological Targeting Diagnosis, Therapy and Rehabilitation, The Fifth Affiliated Hospital, Guangzhou Medical University, No. 621, Gangwan Road, Guangzhou 510700, Guangdong, China. [2]Department of General Practice, GuangDong Engineering Technology Research Center of Biological Targeting Diagnosis, Therapy and Rehabilitation, The Fifth Affiliated Hospital, Guangzhou Medical University, No. 621, Gangwan Road, Guangzhou 510700, Guangdong, China. [3]Department of Cardiology, The First Affiliated Hospital of Bengbu Medical College, Bengbu 233004, Anhui, China. [4]Department of Cardiology, Xijing Hospital, Fourth Military Medical University, Xi'an 710032, China. [5]Department of Urology, GuangDong Engineering Technology Research Center of Biological Targeting Diagnosis,Therapy and Rehabilitation, The Fifth Affiliated Hospital of Guangzhou Medical University, No.621, Gangwan Road, Guangzhou

510700, Guangdong, China. [6]Feng-jin Zhao, Cheng Qin and Li-li Ye contributed equally to this work. ✉email: zhaotg621@126.com; chengqin1016@163.com; doubleliye@163.com

Coronary artery disease (CAD) continues to be a leading global cause of death[1]. It is an inflammatory condition resulting from atherosclerosis, characterized by endothelial dysfunction, lipid accumulation, macrophage activation, and smooth muscle cell proliferation and migration[2], which ultimately leads to lumen narrowing and decreased blood flow to the heart. In the past 20 years, although there have been significant advancements in the diagnosis of CAD, the complex mechanisms underlying the disease still urgently necessitate the identification of better diagnostic biomarkers to enhance clinical treatment and improve patient prognosis.

Endoplasmic reticulum (ER) stress is a cellular state characterized by abnormal protein folding and modification processes in the endoplasmic reticulum, resulting in the accumulation of misfolded proteins[3]. ER stress activates a series of responses known as the ER stress response and is implicated in various diseases, including CAD. Research has shown a strong connection between ER stress and CAD[4–6]. In the arterial vessels of CAD patients, the extent of ER stress may increase due to endothelial cell damage and the presence of inflammatory reactions. ER stress can contribute to the development of CAD through multiple pathways. Firstly, ER stress can cause intracellular calcium imbalance, leading to elevated intracellular calcium levels. This may activate various signaling pathways such as oxidative stress, inflammatory responses, and cell apoptosis, and Unfolded_Protein_Response(UPR), and thereby promoting the formation of atherosclerotic plaques. When cardiomyocytes experience stress from factors like hypoxia, nutrient deficiency, or inflammation, the ER struggles to properly fold newly synthesized proteins, leading to the buildup of unfolded or misfolded proteins. In response to protein accumulation, the UPR is activated to restore normal ER function. However, prolonged UPR activation can trigger the release of pro-inflammatory cytokines like IL-6 and TNF-α, which are linked to atherogenesis and elevated CAD risk. Additionally, ER stress can accelerate plaque formation and progression by influencing lipid metabolism and cholesterol synthesis pathways. Studies have found elevated levels of ER stress-related factors, including IRE1α, PERK, and ATF6, in the plaques of CAD patients[7,8]. These factors regulate the ER stress response and may play a key role in CAD development. In conclusion, ER stress is closely linked to CAD. A better understanding of its role in CAD pathogenesis could reveal new therapeutic targets and improve intervention strategies. Thus, we explored the role of ER stress in CAD and its potential targeted treatments, aiming to identify ER stress genes related to CAD as potential diagnostic biomarkers.

To explore gene alterations in CAD and identify potential biomarkers linked to ER stress, this study integrated two microarray datasets from India and China. The datasets included 16 CAD samples and 14 normal controls, and were analyzed to identify differentially expressed genes (DEGs).

GO and KEGG pathway enrichment analysis were used for functional annotation of CAD-related DEGs, while weighted gene co-expression network analysis (WGCNA) identified co-expressed gene modules[9]. A protein-protein interaction (PPI) network was then constructed using the STRING database to connect the WGCNA and ER stress-related gene sets[10]. Ten hub genes were screened using Cytoscape software from the intercluster DEGs, which were designated as ER stress-related genes (ERSRGs), and a new CAD Gene Expression Risk Score was developed to aid in early CAD detection. Additionally, TF-miRNA-mRNA network was constructed to explore the complex regulatory mechanisms of these genes. DGIdb was used to predict targeted drugs for some ERSRGs. By using the BATMAN-TCM database, it was predicted that the drug most closely associated with ERSRGs is Ginkgo biloba extract (GBE), and the role of GBE was preliminarily validated in cell experiments to depend on the regulation of ER stress. Finally, the regulation of ERSRGs was also validated in single-cell RNA sequencing analysis. This research may offer new perspectives for the diagnosis and treatment of CAD.

Methods

Data collection and processing

Gene expression data of CAD patients were obtained from the GEO database (http://www.ncbi.nlm.nih.gov/GEO)[11,12]. Three datasets (GSE42148, GSE71226, and GSE20681) were selected for next analysis. The detailed information of the selected datasets is presented in Table 1. GSE42148 consists of 13 CAD patients (diagnosed with CAD through quantitative coronary angiography (QCA)) and 11 controls (normal electrocardiogram, no clinical symptoms), based on the GPL13607 platform. GSE71226 comprises 3 CAD patients and 3 controls, based on the Chinese Han population GPL570 platform. The GSE20681 dataset includes 99 CAD patients (≥ 50% stenosis in at least one major vessel) and 99 controls (stenosis < 50%), based on the GPL4133 platform. All data from the three datasets were re-normalized using the ComBat algorithm to eliminate batch effects, and assessed through principal component analysis (PCA). ER stress-related genes were downloaded from the gene cards of gene set enrichment analysis databases (https://www.genecards.org/).Single-cell RNA-seq data includes 1 case of stable CAD and 2 cases of acute coronary syndrome (ACS) (data set numbers GSE184073 and GSE180678). All data sets underwent strict quality control, including filtering out mitochondrial genes and erythrocyte contamination genes, to ensure the reliability of the data.

Identification of differentially expressed genes (DEGs)

Prior to DEG analysis, data preprocessing was performed. Affymetrix in R was utilized for database enhancement through normalization, background correction, and log2 transformation[13]. If a gene has multiple probe locations, the mean value of the probe location values was taken. The "limma" R package[14] was applied to identify DEGs between CAD and control samples in the combined dataset, using |log2 fold change (FC)| > 0.5 and P-value < 0.05 as criteria. Volcano plots were visualized using the "ggplot2" R package, and heatmaps were generated using the "ComplexHeatmap" R package.

GSE dataset	Platform	Organism	Number of Disease	Number of control	Country
GSE42148	GPL13607	Homo sapiens	13	11	India
GSE71226	GPL570	Homo sapiens	3	3	China
GSE20681	GPL4133	Homo sapiens	99	99	USA
GSE184073	GPL24676	Homo sapiens	1	1	Japan
GSE180678	GPL203301	Homo sapiens	1	0	USA

Table 1. The detailed information of the selected datasets.

Functional enrichment analysis

The identified 833 differentially expressed genes were subjected to gene ontology (GO) enrichment analysis and Kyoto Encyclopedia of Genes and Genomes (KEGG)[15–17] pathway analysis using the "clusterProfiler" package in R. For GO analysis, enrichment was evaluated for biological processes (BPs), molecular functions (MFs), and cellular components (CCs). In the enrichment analysis, adjusted $P < 0.05$ was considered statistically significant.

Gene set enrichment analysis (GSEA) and gene set variation analysis (GSVA)

The "clusterProfiler" package[18] in R was utilized to perform gene set enrichment analysis (GSEA)[19] using the "c2.cp.all.v2022.1.Hs.symbols.gmt" (https://www.GSEA-msigdb.org/GSEA/msigdb/index.jsp) reference gene set. Enriched pathways were sequenced based on the false discovery rate (FDR) and normalized enrichment scores (NES). Additionally, significance was determined based on $p < 0.05$ and FDR < 0.05. The results were visualized using the "ggplot2" package in R[20]. GSVA analysis, one of the GSEA algorithms, was conducted to explore pathway differences among different pattern clusters based on enrichment scores. This analysis was performed using the GSVA package (V.1.46.0) in R[21]. In this study, GSVA analysis was performed on each marker gene. The "h.all.v2023.1.Hs.symbols.gmt" and "c2.cp.ractme.v2023.2.Hs.symbols.gmt" gene sets were downloaded from the MsigDB database for analysis. Differential analysis was carried out using the limma package in R, where a P-value < 0.05 indicated statistical differences between the CAD and control groups.

Weighted gene correlation network analysis (WGCNA)

The WGCNA program package[9] in R was applied to identify co-expressed gene modules, examine the relationship between gene networks and phenotypes, and investigate core genes within the network. WGCNA was performed on the DEGs between CAD and control datasets.Firstly, hierarchical clustering analysis was employed to select discrete cases. Then, an optimal soft power value (β) was determined to build a weighted adjacency matrix, which was then converted into a topological overlap matrix (TOM) with module assignments marked by color and module eigengene (ME) characteristics. The "minModuleSize" was set to 50, and module significance and correlation coefficients were calculated among different modules. Finally, the most relevant modules associated with the disease were identified, and feature genes were extracted for subsequent analysis.

Analysis of protein–protein interactions (PPI) and identification of ERSRGs

The hub genes within the module showing the highest correlation with CAD were selected from WGCNA. ERSRGs were identified by overlapping the hub genes, ERGs, and DEGs through a Venn diagram. Subsequently, the "pROC" R package was employed to perform ROC analysis and evaluate the diagnostic effectiveness of ERSRGs for CAD. To explore the interactions among ERSRGs, a protein-protein interaction network was built using the STRING database (version 12.0, http://string-db.org))[22]. Unconnected nodes were removed, and the network was visualized in Cytoscape software (version 3.10.1, https://cytoscape.org)[23]. Key gene clusters were identified using the MCODE plugin, with the cluster scoring 7.333 being visualized.

Correlation analysis

The expression correlation of 10 ERSRGs in all samples and CAD samples was calculated. The correlations were performed by Pearson's correlation analysis using rcorr function in the "hmisc" R packageand visualized with using the "corrplot" R package..

Immune infiltration analysis

CIBERSORT[24] was used to analyze the proportions of different immune cell types based on gene expression data. The R software CIBERSORT was employed to analyze the gene expression matrix data, combined with the LM22 signature gene matrix, and samples were filtered with $P < 0.05$ to obtain an immune cell infiltration matrix. For each sample, the sum of all evaluated immune cell type components equals 1[25].

Construction and validation of the scoring model

Merge three datasets (GSE42148, GSE71226, and GSE20681) and implement an 80% and 20% split for the training set and validation set, respectively. To ensure biological relevance while maintaining statistical rigor, we implemented a two-level feature selection strategy. First, we identified the top 3 differentially expressed genes in the extended training set. Simultaneously, from the original 10 hub genes, we selected TLR2 and MMP9, which have established roles in cardiovascular pathophysiology and endogenous stress responses. Finally, we identified five stable biomarkers: L1TD1, EGR3, CXorf36, TLR2, and MMP9, which are statistically robust and biologically reasonable. We also employed regularized logistic regression training models and 10-fold cross-validation during model training to optimize parameters and reduce overfitting. Calibration curves were used to

assess the fit between actual values and predicted values. Receiver Operating Characteristic (ROC) curves and the area under the ROC curve (AUC) were used to further evaluate the predictive ability of the model.

TF-miRNA-mRNA regulatory network analysis

To further understand the regulatory mechanisms of central genes and explore upstream regulatory factors, we obtained transcription factor (TF)-target interactions through text mining based on sentences using the Transcriptional Regulatory Relationships Unraveled by Sentence-based Text mining (TRRUST) database[26]. TRRUST is a database that predicts transcriptional regulatory networks and includes regulatory relationships between transcription factors and their target genes. We predicted the target miRNAs (miRNAs) of ERSRGs using the miRWalk[27] and miRDB[28] databases. The miRNAs identified in both databases were considered as the target miRNAs of ERSRGs in CAD. We constructed miRNA-mRNA and mRNA-TF interaction networks using Cytoscape.

Construction of target gene–drug networks and validation of GBE

The Drug-Gene Interaction Database (DGIdb) version 3.0[29] is an open-source project that assists users in mining existing resources and generating hypotheses on how genes can be used as drug development targets. Key genes considered as potential drug targets for treating CAD were input into DGIdb to explore existing drugs or small organic compounds. We selected the top 30 drugs for CAD treatment. The results were visualized using the "ggplot2 (3.2.1)" and "ggalluvial (0.11.1)" R packages.

Using the BATMAN-TCM database to predict the traditional Chinese medicine components that bind most closely with ERSRGs, the combination of ERSRGs and Ginkgo folium is the closest. To conduct experimental validation, H9c2 cells were placed in a 1% O_2 hypoxic incubator to create a hypoxia model, 4-phenylbutyric acid (4-PBA, 10μM) was used to inhibit ERs, tunicamycin (EMD, 1 μg/mL) was used to induce ERs, and Ginkgo flavonoids (2 μM) were used for intervention treatment.

Single-cell RNA sequencing analysis

In this study, we used the Seurat R package to process single-cell RNA sequencing (scRNA-seq) data, removing doublets and retaining cells with less than 20% mitochondrial genes, more than 300 total genes, more than 1000 expression levels, and genes expressed in at least 3 cells. The number of highly variable genes was set to 3000. Subsequently, we employed principal component analysis (PCA) and uniform manifold approximation and projection (UMAP) techniques for dimensionality reduction and visual analysis of the data. Based on specific marker genes, we divided the cells into five different populations: Fibroblasts, Lymphocytes, Macrophages, Monocytes, BCells. Further analysis focused on the expression distribution of ERSRGs in each cell population.

Real-time quantitative PCR

Specimens were collected from three patients diagnosed with CAD at the First Affiliated Hospital of Bengbu Medical College and three healthy individuals from a routine health examination(From June 1st to July 1st, 2023). The study was conducted in accordance with the Declaration of Helsinki, and the protocol was approved by the Ethics Committee of The First Affiliated Hospital of Bengbu Medical College on April 26, 2023 (Ethics code: 2023YJS117, in item 117 of the document "Notice on the Issuance of Ethical ApprovalResults of 2022 Graduate Project Projects").The study has obtained informed consent from the participants and signed the informed consent form.Total RNA of blood samples from both CAD patients and controls was extracted using TRIzol Reagent (Life Technologies, CA, USA). After quantifying and assessing the purity of the RNA, reverse transcription was performed using the sweScript RT I First strand cDNA Synthesis All-in-OneTM First-Strand cDNA Synthesis Kit (ServiceBio, Wuhan, China). Subsequently, qPCR was carried out using the 2×Universal Blue SYBR Green qPCR Master Mix (ServiceBio, Wuhan, China) under the following thermal cycling conditions: 95 °C for 60 s, 95 °C for 20 s, 55 °C for 20 s, and 72 °C for 30 s. The gene expression was calculated using the 2-ΔΔCt method. The primer sequences used in this study are listed in Table 2.

Statistical analysis

R (version 4.1.3) was utilized for statistical analysis. A P-value < 0.05 was set as a significance threshold for screening DEGs, immune infiltration analysis, immune-related gene model, qPCR, and drug prediction.

Results

Data pre-processing

The flow of this study was shown in (Fig. 1A). The GSE42168 and GSE71226 datasets were obtained from the GEO repository and normalized in R. After merging the datasets, we ensured that the batch effect was eliminated. As shown in Fig. 1B and D, there were noticeable differences between and within groups before batch effect removal, which were corrected after eliminating the dataset source's batch effect (Fig. 1C and E). A total of 30 samples were included in the study, with patients categorized into a control group (luminal stenosis < 50%) and a CAD group (≥ 50% stenosis in at least one major vessel) based on the degree of coronary artery stenosis (Table 1).

Identification of DEGs

Differential expression analysis between CAD and control samples in the merged GSE42148 and GSE71226 dataset was performed using the "Limma" package in R 4.2.2. A total of 833 DEGs were identified, with 507 genes upregulated and 326 downregulated (log2FC > 0.05 and P-value < 0.05). The DEGs were visualized in a volcano plot (Fig. 2A), where downregulated genes are shown in green, upregulated genes in red, and others in grey. The top 20 upregulated and downregulated genes are displayed in Fig. 2B.

Target gene	Primer(5'-3')		Size(bp)
β-ACTIN	Forward primer: GCTTCTTTGCAGCTCCTTCG Reverse primer: GGCCTCGTCACCCACATAG		224
AZU1	Forward primer: ATGCCCGCTTCGTGATGAC Reverse primer: CTGATGGAAAACGTCTGGCG		127
CAMP	Forward primer: AGGTCCTCAGCTACAAGGAAG Reverse primer: TCTTGAAGTCACAATCCTCTGGT		210
ELANE	Forward primer: CTCGCGTGTCTTTTCCTCG Reverse primer: GCCGACATGACGAAGTTGG		185
LTF	Forward primer: ATGGTGGTTTCATATACGAGGCA Reverse primer: CTTTCGGTCCCGTAGACTTCC		79
MMP8	Forward primer: TGCTCTTACTCCATGTGCAGA Reverse primer: TCCAGGTAGTCCTGAACAGTTT		85
MMP9	Forward primer: TGTACCGCTATGGTTACACTCG Reverse primer: GGCAGGGACAGTTGCTTCT		97
MPO	Forward primer: TGCTGCCCTTTGACAACCTG Reverse primer: TGCTCCCGAAGTAAGAGGGT		142
PPARG	Forward primer: GGGATCAGCTCCGTGGATCT Reverse primer: TGCACTTTGGTACTCTTGAAGTT		186
TLR2	Forward primer: ATCCTCCAATCAGGCTTCTCT Reverse primer: GGACAGGTCAAGGCTTTTTACA		118
TLR8	Forward primer: ATGTTCCTTCAGTCGTCAATGC Reverse primer: TTGCTGCACTCTGCAATAACT		143

Table 2. The primer sequences used in this study.

Function and pathway enrichment analyses

We conducted GO enrichment analysis and KEGG pathway enrichment analysis to further investigate the possible biological roles of DEGs. The results of the analysis indicated that these DEGs were largely involved in several biological activities, including neutrophil-mediated killing of symbiont cell, neutrophil mediated cytotoxicity, and cell killing (Fig. 3A).Additionally, Fig. 3C illustrates the enriched pathway genes, including ELANE, AZU1, and LTF, which are implicated in these pathways. These biological processes highlight the significance of inflammatory responses and immune regulation in the pathogenesis of CAD, suggesting that neutrophils may play a critical role in the development and progression of CAD. KEGG pathway enrichment analysis further elucidated the potential biological functions of the DEGs. The analysis revealed that these genes are enriched in several key pathways: herpes simplex virus 1 infection, IL-17 signaling pathway, and autophagy - animal (Fig. 3B, D) presents the KEGG-enriched pathway genes, including TLR2 and MMP9, which contribute to the enrichment of these pathways. The IL-17 signaling pathway plays an important role in inflammatory responses, potentially contributing to the formation of the inflammatory microenvironment associated with CAD by promoting the aggregation and activation of inflammatory cells. Autophagy, on the other hand, serves a protective role in cellular stress responses, facilitating the clearance of misfolded proteins and maintaining cellular homeostasis. The autophagic mechanisms triggered by ER stress may exert protective effects in the pathological process of CAD and warrant further investigation. Overall, this series of analyses identified 833 differentially expressed genes that not only exhibited significant expression changes in disease but also demonstrated strong associations with histopathological inflammation.

We subsequently performed GSEA to assess the impact of gene expression levels on CAD. Figure 4A displays the top ten enriched pathways. The GSEA results revealed that DEGs are strongly linked to several important gene sets. Specifically, pathways like "Neutrophil Degranulation" and "NGF Stimulated Transcription" showed significant enrichment, indicating that immune responses and nerve growth factor signaling may be crucial in the development and progression of CAD. Conversely, pathways related to "Mitochondrial Translation" and "Translation" were significantly downregulated, indicating that these processes may be suppressed in the context of CAD (Fig. 4B–F). To validate the results of the gene set enrichment, we employed GSVA. This method transformed the gene expression matrix across different samples into a matrix of gene set expressions, allowing us to evaluate the enrichment of various metabolic pathways. The results were visualized using the pheatmap package (Fig. 4G, H). Figure 4G shows the GSVA analysis based on "h.all.V2023.1.Hs.symbols.gmt", while Fig. 4H shows the GSVA analysis based on "c2.cp.ractme.V2023.2.Hs.symbols.gmt".The GSVA analysis further corroborated our findings, revealing differences in gene expression profiles and metabolic pathways among samples, particularly highlighting the significant enrichment of the UPR pathway associated with ER stress. The UPR aids cells in responding to adverse environmental conditions and restoring ER function. This result not only underscores the importance of ER stress in the pathogenesis of CAD but also provides potential targets for identifying new biomarkers. By comparing gene expression across different groups, we can identify key signaling pathways that may be activated in CAD patients, thereby offering a theoretical basis for subsequent clinical research and therapeutic strategies.

Identification of ERSRGs in CAD

We constructed a co-expression network using WGCNA for normal controls and CAD patients, identifying key gene modules associated with CAD. When the soft threshold parameter β was set to 6 and $R^2 > 0.9$, a scale-

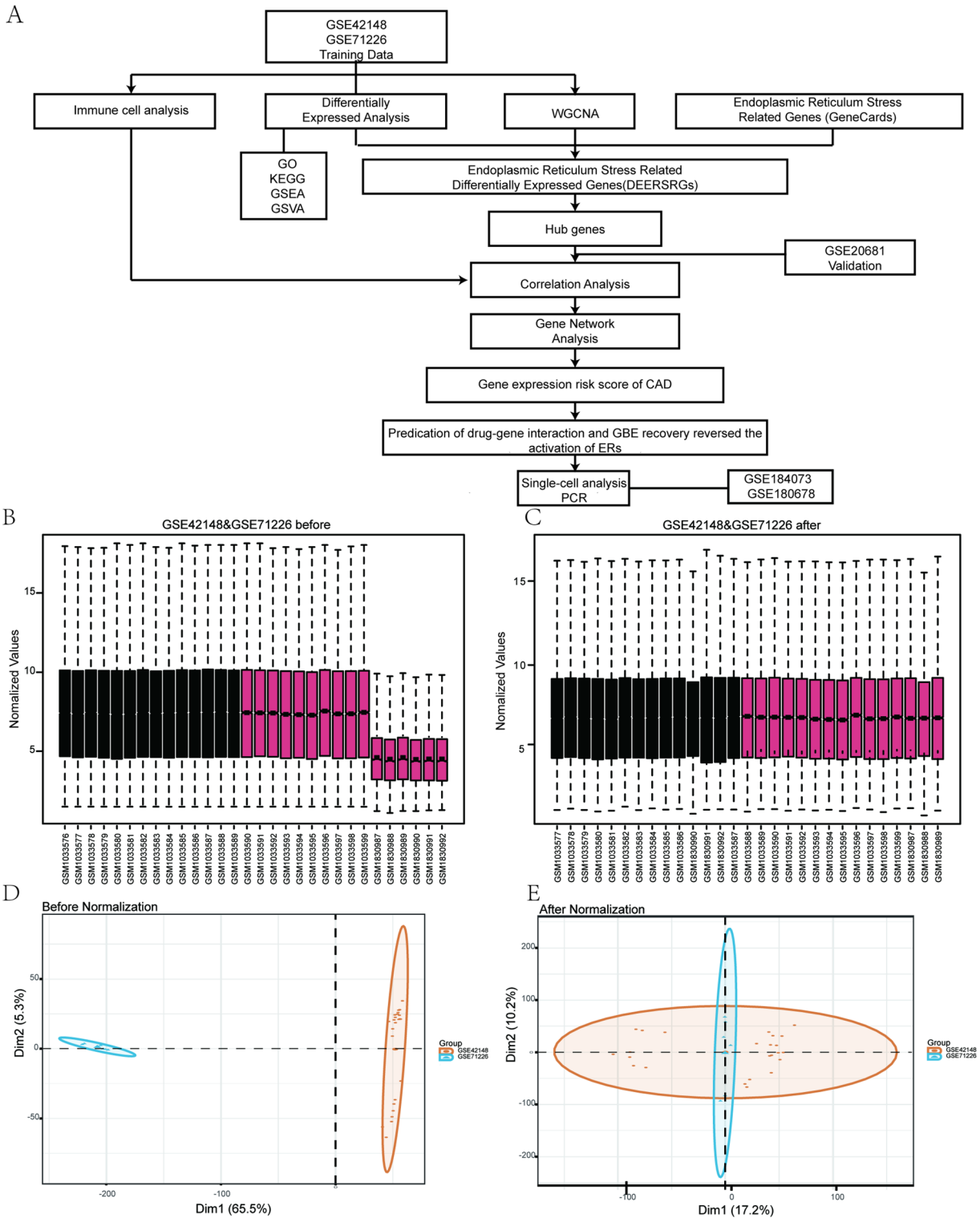

Fig. 1. Flow chart and boxplots of consolidated datasets before and after removing batch effects. (**A**) Flow chart of methodologies applied in this study. (**B**) Box line diagram of the merged datasets before correction. (**C**) Box line diagram of the combined datasets after correction. (**D**) PCA for CAD and healthy control samples before batch correction with ComBat. (**E**) PCA for CAD and healthy control samples after batch correction with ComBat.

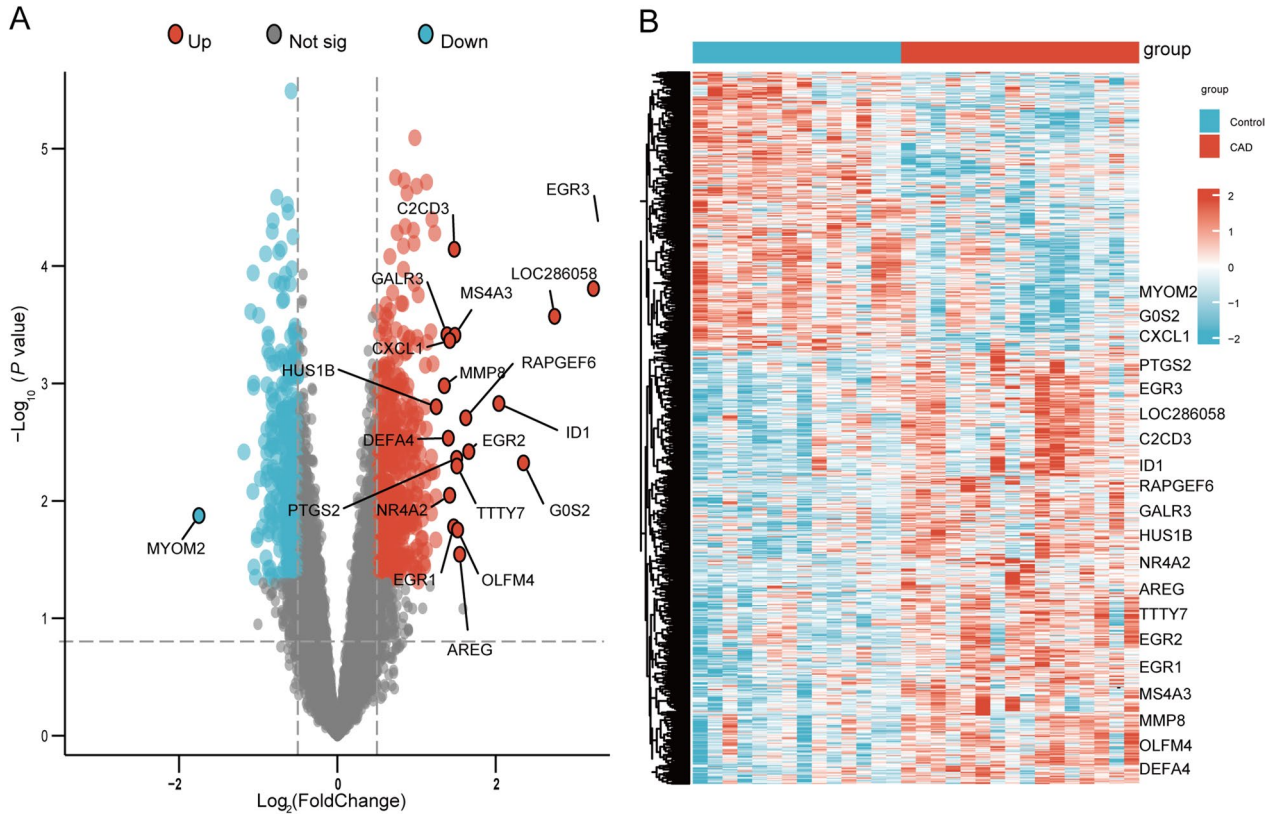

Fig. 2. DEGs analysis between the CAD and control in merge data (GSE42148 and GSE71226 datasets) cohort. (**A**) Volcano plot of DEGs constructed; red dots represent up-regulated differential genes, grey dots represent nonsignificant genes, and green dots represent down-regulated differential genes. (**B**) Heatmap plot of DEGs. Different colors represent the trend of gene expression in different tissues.The red and blue swatches represent upregulated and downregulated DEGs, respectively.

free network was constructed under this condition (Fig. 5A). Strongly correlated modules were merged with a clustering height threshold of 0.5 (Fig. 5B), resulting in the identification of 23 modules for further analysis. In Fig. 5C, the induced and merged modules are presented as a clustering dendrogram. Furthermore, we analyzed the co-expression similarity and continuity of clinical characteristics (normal controls and CAD) using genes from these 23 modules. We found that the bisque4 module exhibited the strongest association with CAD ($r = 0.44$, $p = 0.02$), containing 1,457 hub genes (Fig. 5D).

To refine the ERSRGs, we identified 94 genes by using Venn diagrams to find common genes across ER stress, DEmRNA, and hub genes (Fig. 6A). A PPI network was then built using the STRING database to explore their interactions. Two cluster modules were detected with the MCODE plugin, where cluster 1 had the highest score (7.333, 10 nodes, and 33 edges). In total, 10 hub genes were identified (Fig. 6B and C).

We also assessed the correlations between ERSRGs and observed notable synergistic effects in both all samples and CAD samples (Fig. 6D and E).Most genes exhibited correlation coefficients greater than 0.5, particularly ELANE and AZU1, which showed a strong positive correlation (Cor = 0.98). This strong correlation among hub genes suggests that they may be co-regulated by the same transcription factors, participate in the same biological processes or signaling pathways, and potentially perform complementary or synergistic functions within the cell. Figure 6F displays the expression patterns of the 10 ERSRGs in the CAD group versus healthy controls. We then conducted ROC analysis to assess the diagnostic value of these ERSRGs (Fig. 6G). All genes showed AUC values greater than 0.72, with TLR2 having the highest AUC (0.853,CI: 0.692–1.000) and ELANE the lowest (0.728, CI ˙ 0.536–0.920).

Immune landscape analysis

Much pieces of evidence indicates a close relationship between the immune microenvironment and CAD[30–32]. Therefore, we utilized the CIBERSORT algorithm to calculate the relative abundance of 22 immune cells in each CAD and normal sample (Fig. 7A). To validate the role of the immune microenvironment in the pathogenesis of CAD, we performed differential analysis of immune cell abundance between the CAD group and the normal group and conducted correlation analysis between marker genes and the 22 immune cells. The results indicated that the infiltration levels of memory B cells ($P = 0.048$) and resting NK cells ($P = 0.013$) were significantly higher in CAD patients than in the normal control group (Fig. 7B). The interactions among these immune cells further support the important role of the immune microenvironment in CAD pathogenesis. Additional analysis of immune cell infiltration in CAD revealed several correlations between these cells (Fig. 7C). We also conducted

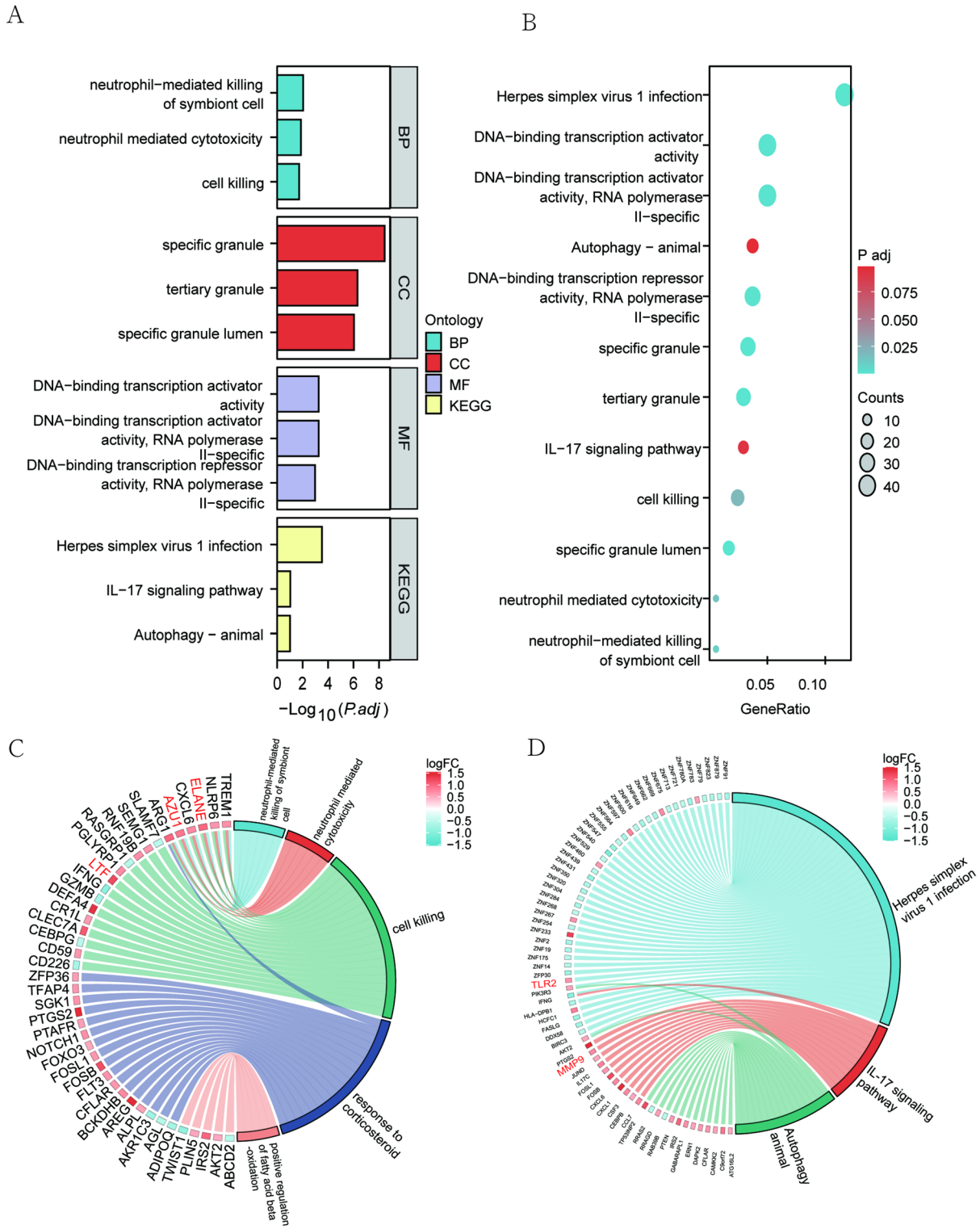

Fig. 3. GO and KEGG enrichment analyses of DEGs. (**A**) The enriched GO terms of DEGs. BP biological process, CC cellular component, MF molecular function. (**B**) The enriched KEGG terms of DEGs. (**C**) GO enrichment analyses of DEGs. (**D**) KEGG enrichment analyses of DEGs.

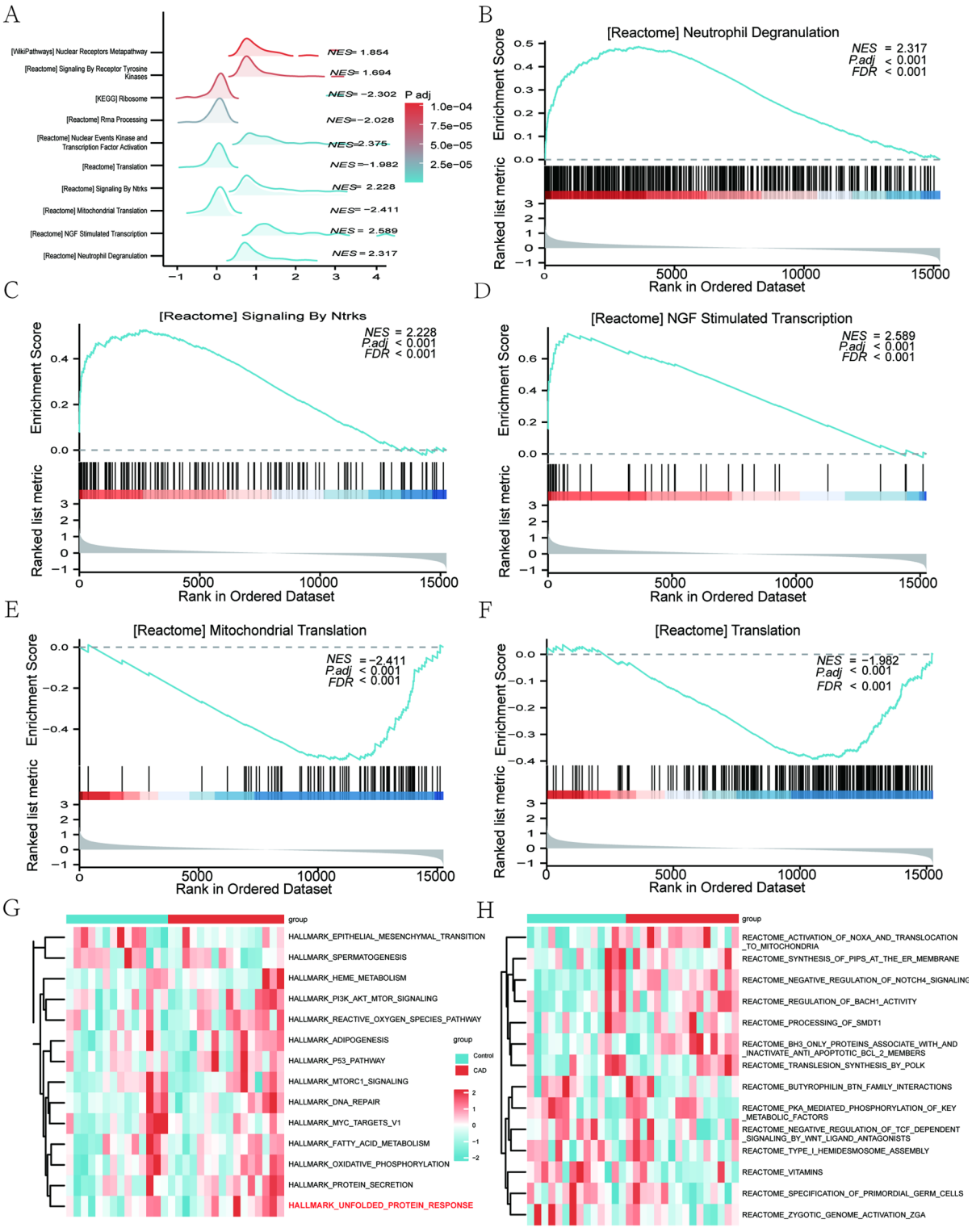

Fig. 4. Results of GSEA and GSVA. (**A**) Mountain range plot showing the GSEA results of the merged dataset. Horizontal coordinate shows the gene ratio, vertical coordinate show the c2 pathways, and the color indicates P-value. (**B**–**F**) The top 5 items of the GSEA. (**G**,**H**) Heat map showing the results of GSVA. G shows the GSVA analysis based on "h.all.V2023.1.Hs.symbols.gmt", while H shows the GSVA analysis based on "c2.cp.ractme. V2023.2.Hs.symbols.gmt".Red and blue indicate activation and suppression, respectively.

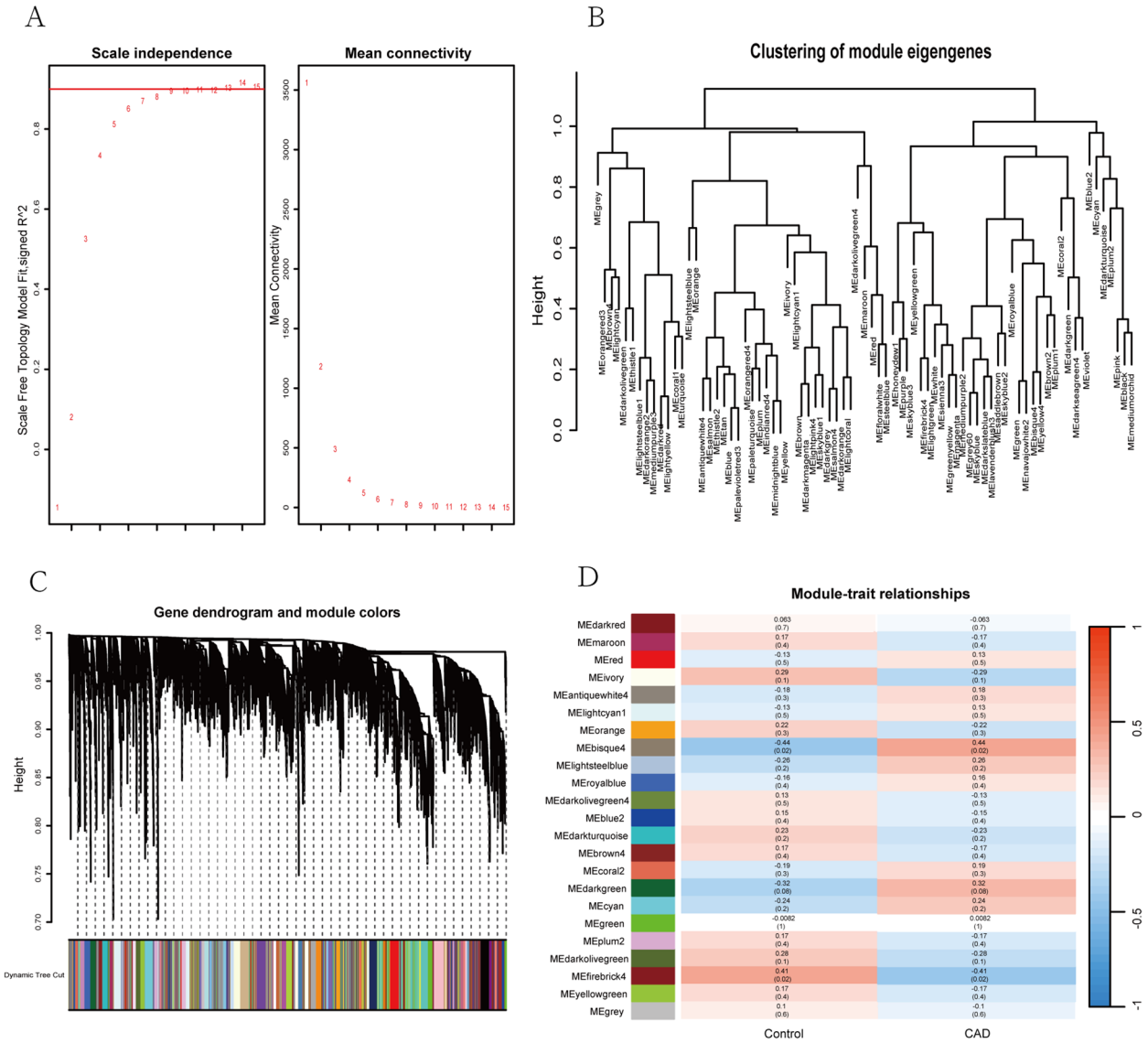

Fig. 5. Identification of modules associated with CAD. (**A**) Scale-free index analysis for soft-threshold power and mean connectivity analysis for various softthreshold powers. (**B**) The cluster tree dendrogram of co-expression modules is shown in different colors. (**C**) Cluster analysis of the combined dataset. The different module clusters are color-coded. (**D**) Heatmap of the correlation between module eigengenes and CAD.

correlation analysis between hub genes and the 22 immune cells (Fig. 7D). Correlation analysis revealed that Macrophages M0 were significantly positively correlated with the genes MMP9 ($r = 0.495$, $P = 0.005$) and PPARG ($r = 0.376$, $P = 0.041$). In contrast, B cells memory exhibited a negative correlation with AZU1 ($r = -0.500$, $P = 0.005$) and several other marker genes. These findings suggest that alterations in the immune microenvironment of patients with CADe may be closely related to genes such as MMP9, MMP8, and PPARG, indicating that ER stress may play a critical role in this process.

Gene expression risk score of CAD

By integrating multiple datasets (GSE42148, GSE71226, and GSE20681) and a rigorous feature selection strategy, we established a CAD gene expression risk score based on 5 gene markers (L1TD1, EGR3, CXorf36, TLR2, MMP9). This scoring model demonstrated excellent discriminative ability on the independent validation set (AUC = 0.791) (Fig. 8C), showing improved generalization capability while maintaining a certain predictive performance. Notably, the performance of the validation set was slightly better than that of the training set (AUC = 0.694) (Fig. 8A), indicating a better balance between fitting and generalization. The calibration plot also showed good calibration performance of the model (Fig. 8B, D). The model is visualized using a nomogram, where each gene corresponds to a score, and the total score is calculated by summing the scores of all genes. Different total scores correspond to different risks of coronary artery disease (Fig. 8E).

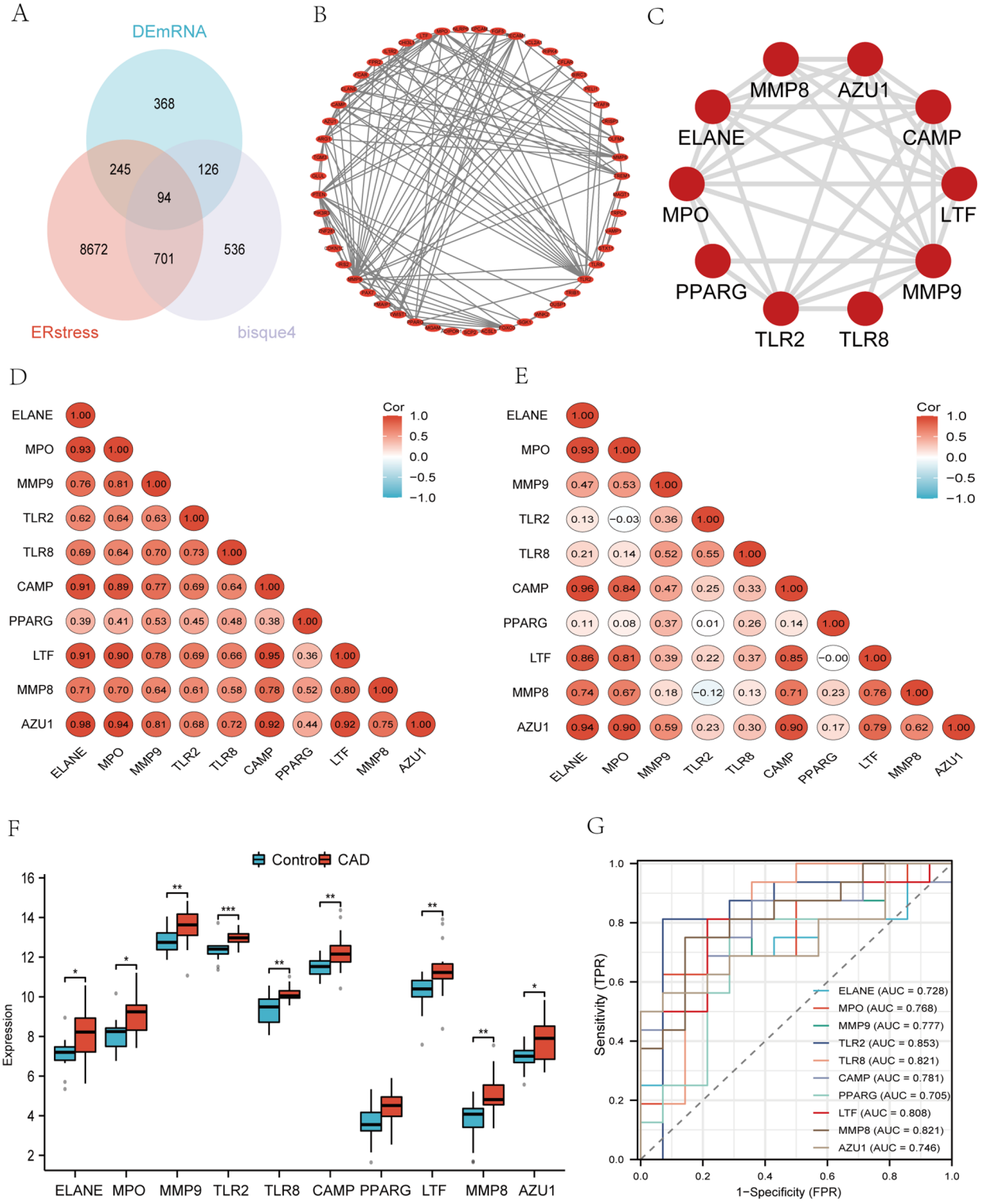

Fig. 6. Identification of ERSRGs. (**A**) Venn diagram showed the overlapping genes between DEmRNA, ERGs, and the genes of the bisque4 module. (**B**) MCODE was used to identify hub genes in the protein interaction network of ERSRGs. (**C**) MCODE sub-network. (**D**) Correlation analysis of ERSRGs in all samples. (**E**) Correlation analysis of ERSRGs in CAD samples. (**F**) Group comparison chart, displaying the expression differences of ERSRGs between CAD patients and healthy control groups in the merged dataset. (**G**) ROC curves of ERSRGs in the merged dataset. ERGs, endoplasmic reticulum stress genes; ERSRGs, endoplasmic reticulum stress-related genes; ROC, receiver operating characteristic. $^{*}p < 0.05$, $^{**}p < 0.01$,$^{***}p < 0.001$.

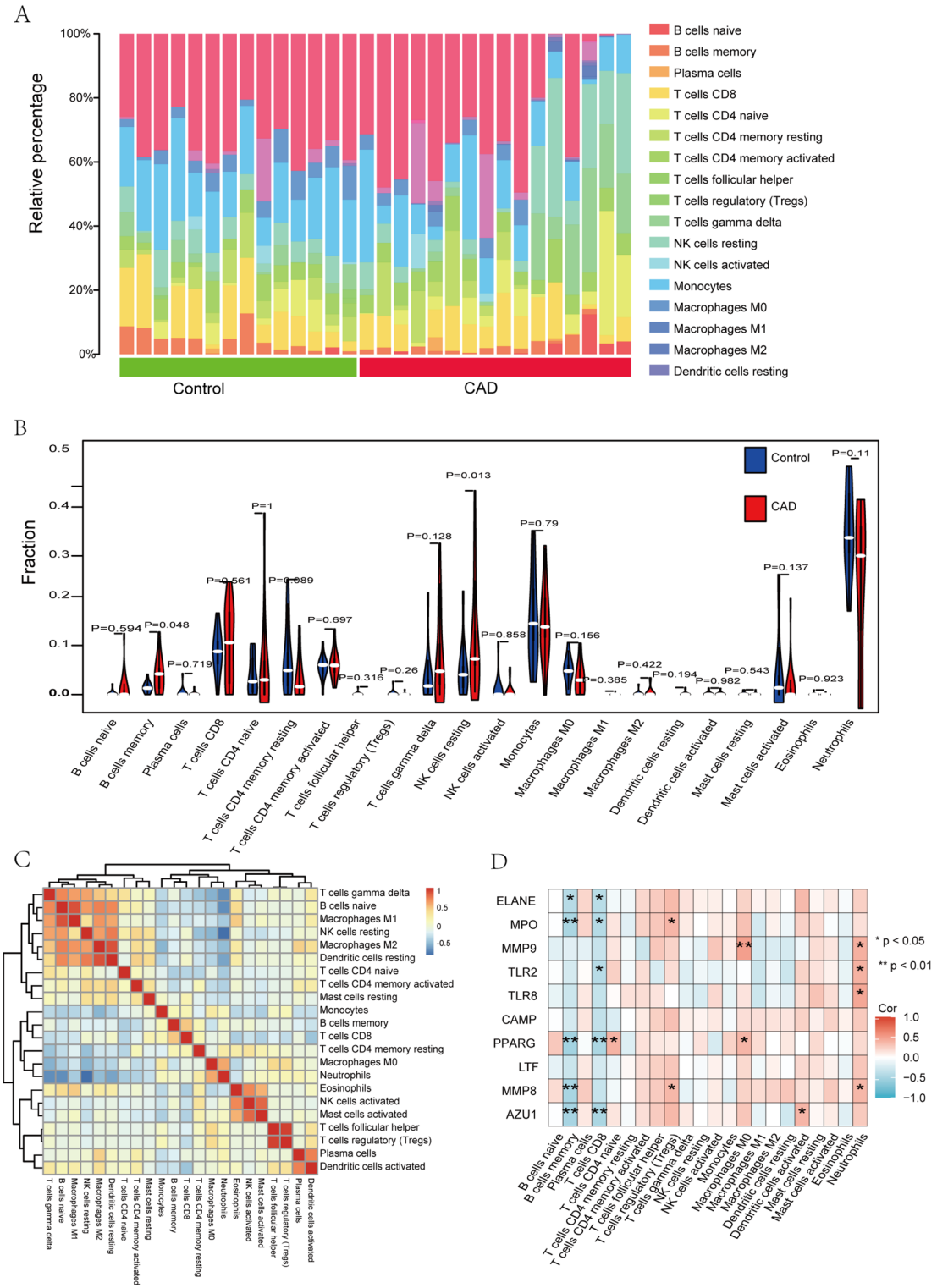

Fig. 7. The immune characteristics between the CAD group and healthy controls in the merged dataset. (**A**) Histogram showing the distribution of 22 immune cells infiltration between the CAD group and healthy control. (**B**) Boxplot showing the differences in infiltrated immune cells between the CAD group and healthy controls. (**C**) Heatmap delineating the correlation in immune cell infiltrations. Blue and red indicate positive and negative correlations, respectively. The darker the color the stronger the correlation. (**D**) Correlation of ERSRGs and 22 immune cell types. $*p < 0.05$, $**p < 0.01$.

Construction of TF-miRNA-mRNA Networks and validation of ERSRGs

Building on the ERSRGs from our previous study, we further explored their regulatory interactions with other small molecules, including relationships with TFs and miRNAs (Fig. 9A). TF targets of ERSRGs in CAD were predicted using the TRRUST database, while miRNA targets were identified through the miRWalk and miRDB databases. miRNAs found in both databases were considered ERSRG-targeting miRNAs in CAD. We constructed TF-miRNA-mRNA network using Cytoscape. The network consists of 55 nodes (8 marker genes, 39 miRNAs, and 8 TFs) and 77 edges. A total of 39 miRNAs were predicted as targets by 8 ERSRGs in CAD, and 2 genes (CAMP, Azu1) were not predicted as target miRNAs. 6 ERSRGs predicted 8 TFs in CAD, while TLR8, CAMP, MMP8, AZU1 did not predict any TF.

To further validate the involvement of the core UPR signaling pathway, we performed GSEA analysis using the established HALLMARK_UNFOLDED_PROTEIN_RESPONSE gene set. The results confirmed that the UPR pathway is significantly activated in CAD patients (Fig. 9B, NES = 1.454, FDR = 0.0135), providing a solid foundation for the involvement of ER stress.

We then quantified UPR activity in each sample using GSVA. Notably, the expression levels of most hub genes (Fig. 9C, TLR8, $r = 0.719$, $p < 0.001$; MMP9, $r = 0.718$, $p < 0.001$) showed a strong positive correlation with UPR activity scores, indicating that these genes are not only inflammatory markers but also closely linked to the core ER stress response in CAD.

Furthermore, we observed a significant co-expression pattern between the identified ERSRGs and key mediators of the UPR branches, with the expression of TLR2, TLR8, ELANE, AZU1, etc., significantly correlated with CHOP (DDIT3), EIF2S1, ERN1, etc. (Fig. 9D), suggesting that they are part of the same functional pathway.

Predication of drug-gene interaction and GBE recovery reversed the activation of ERs

In order to initially explore the treatment of CAD, the DGIdb database was used to predict potential gene-targeted drugs. A total of 177 drugs or compounds targeting 10 ERSRGs were identified. The top 30 drugs/compounds are displayed in Fig. 10 according to the order of "interaction score" from the DGIdb database. Among them, the first 4 drugs targeted TLR2 and TLR8, of which the interaction score was as high as 30.91, and 121 drugs targeted PPARG, resulting in the most targeted drugs.No potential drugs could be identified for CAMP and AZU1.

Using the BATMAN-TCM database, it was predicted that ERSRGs have the closest binding with Ginkgo folium (Table 3), confirming GBE as the preferred candidate drug targeting our ER stress-related genes. Experimental validation showed that Ginkgo treatment significantly improved ER stress in cardiac muscle cells (Fig. 11A-D). After 24 h of GBE treatment in H9c2 cardiomyocytes, Western blot detection revealed that the ER stress markers CHOP and BiP, ATF4 were significantly downregulated ($P < 0.05$), suggesting that GBE may alleviate ER stress by inhibiting the UPR pathway. The expression of CHOP, BiP and ATF4 in the GBE + 4-PBA group was lower than that in the GBE monotherapy group, indicating that the inhibition of ER stress synergizes with GBE, suggesting that the effect of GBE depends on ER stress regulation. The expression of CHOP, BiP and ATF4 in the GBE + EMD group rebounded, indicating that ER stress activation can partially counteract the protective effect of GBE, further supporting its mechanism dependence. The multi-target action of Ginkgo folium explains its potent regulation of ER stress, providing a new CAD treatment strategy through targeting the ER stress pathway.

The expression of the identified top 10 ERSRGs

Finally, qRT-PCR was performed to validate the potential target genes(ERSRGs) mentioned above. As shown in Fig. 12A-C, we examined the expression of these genes in CAD patients and healthy controls using the GSE42148, GSE71226, and GSE20681 datasets. Most of the genes showed higher expression in CAD samples. In the GSE42148 dataset, the expression of AZU1, LTF, MMP8, MPO, PPARG, TLR2, and TLR8 was significantly upregulated in CAD patients ($p < 0.05$). In the GSE71226 and GSE20681 datasets, the expression of MMP9 was significantly upregulated in CAD patients ($p < 0.05$). Subsequently, we examined the expression levels of these genes in CAD patients ($n = 3$) and healthy controls ($n = 3$), and found that compared to the healthy control group, CAD patients exhibited significant upregulation of LTF, MMP8, MMP9, and TLR2 mRNA expression ($p < 0.05$) (Fig. 12D). Our experimental results were largely consistent with the data analysis. Expression data for ELANE was not detected in the GSE20681 dataset.

Single-cell analysis of ERSRGs

Due to the differences in cell composition that may confound transcriptomic analysis in whole blood studies, we conducted single-cell RNA sequencing analysis to directly address the issue of cell heterogeneity. We utilized the GSE184073 and GSE180678 scRNA-seq datasets to elucidate the inherent cellular heterogeneity present in CAD, which were derived from one patient with stable coronary artery disease and two patients with acute coronary syndrome. We first performed quality control on the single-cell dataset, restricting the percentage of mitochondrial genes and erythrocyte genes to ensure the reliability of the cell samples. Then, we clustered all cells into 10 clusters using the KNN clustering algorithm (Fig. 13A). Based on the surface marker genes of different cell types, we observed their expression in different clusters (Fig. 13C), and we annotated a total of five different cell types, including Fibroblasts, Lymphocytes, Macrophages, Monocytes, and B-Cells (Fig. 13B). We defined stable coronary artery disease as the control group and acute coronary syndrome patients as the disease group. The 10 characteristic genes identified in our previous study were mainly distributed in Macrophages and Monocytes (Fig. 13D), indicating that hub genes may play a central role in the immune regulation, inflammatory response, and immune response of Monocytes and Macrophages. The proportions of these five cell types were observed to differ between the two groups (Fig. 13E). Furthermore, we found that the two key hub genes, TLR2 and TLR8, were primarily expressed in Monocytes, with very little expression in other immune cell

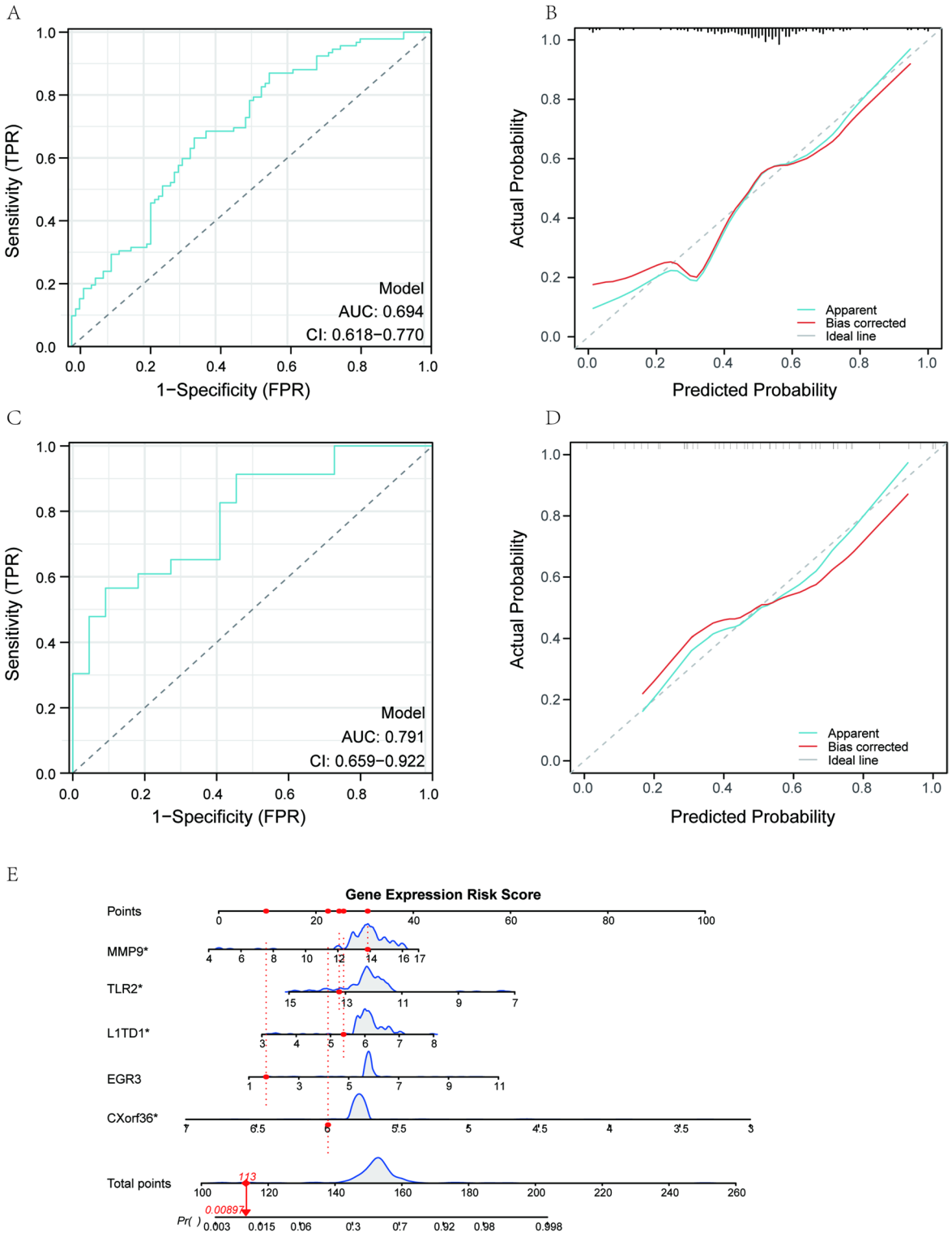

Fig. 8. Construction and validation of the scoring model. (**A**) Gene expression in the ROC curve for CAD diagnosis. (**B**) Calibration curve of the training set. (**C**) ROC curve for CAD in the validation set. (**D**) Calibration curve of the validation set. (**E**) Risk scoring model of gene expression for CAD.

types. Hypergeometric testing revealed that our hub genes were significantly enriched in Monocytes (Fig. 13F, FDR = 0.009, enrichment ratio = 3.7), indicating that these genes are mainly expressed in Monocytes and are related to Monocyte function. There was a lack of significant enrichment in other cell types (Macrophages: FDR = 0.209; Fibroblasts: FDR = 0.812; other cells: FDR = 1.000), suggesting that our findings have significant specificity for the Monocyte region. This upregulation of Monocyte specificity is entirely consistent with the

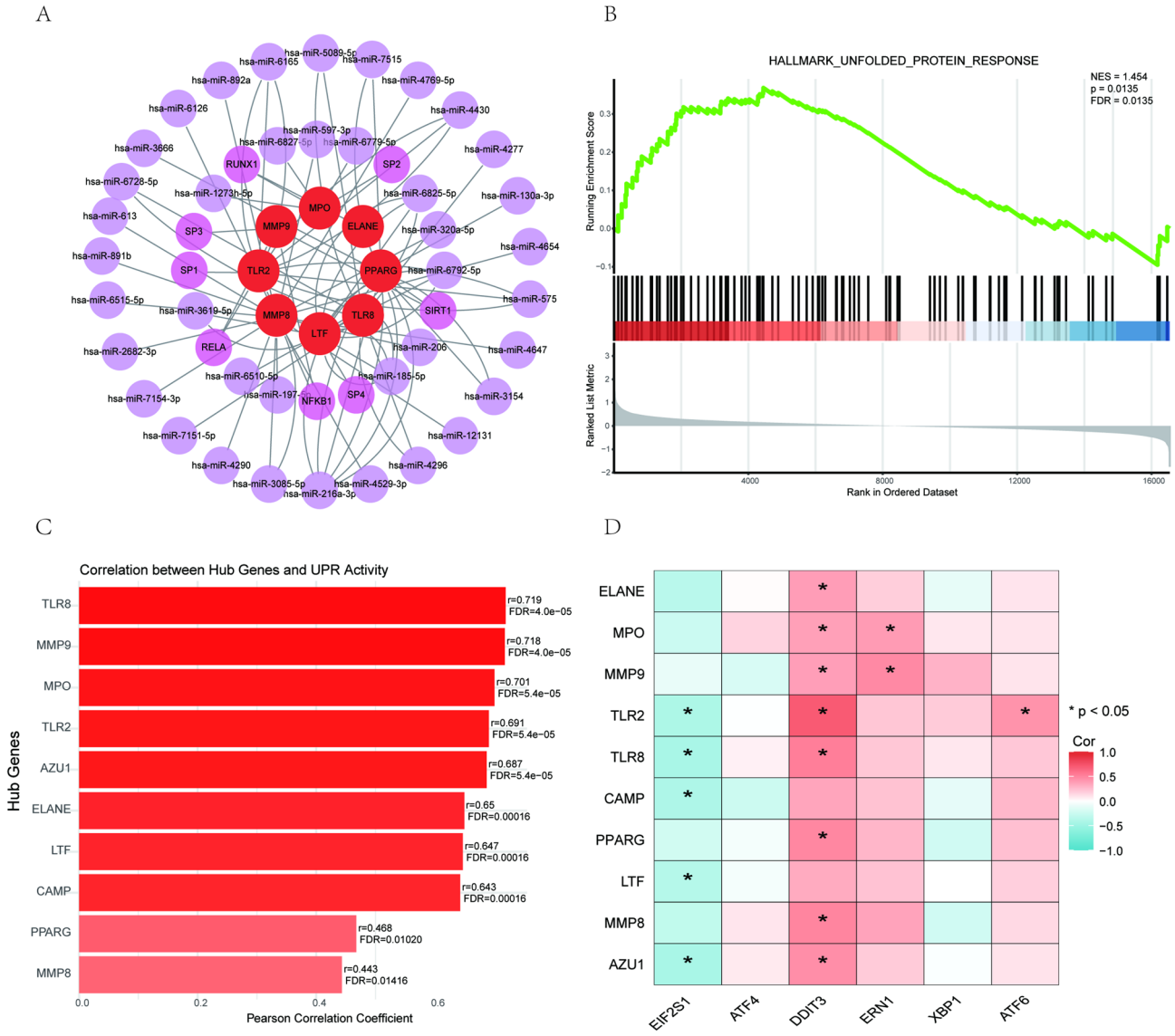

Fig. 9. TF-miRNA-mRNA network and functional validation based on ERSRGs. (**A**) TF-miRNA-mRNA network, red represents ERSRGs, rose red represents transcription factors, pink represents miRNA. (**B**) Pathway enrichment of UPR. (**C**) Correlation between ERSRGs and UPR activity. (**D**) Correlation between the expression of ERSRGs and UPR core molecules.

established pathophysiology of CAD, where Monocyte-derived Macrophages play a central role in plaque inflammation and progression.

Discussion

CAD is a common cardiovascular disorder primarily caused by atherosclerosis of the coronary arteries, leading to pathological changes such as myocardial ischemia, hypoxia, and necrosis. With changes in lifestyle and an aging population, the incidence of CAD continues to rise, posing a significant global public health problem. Currently, CAD diagnosis and treatment are constrained by existing technologies. Diagnosis mainly depends on coronary angiography, which can delay treatment for patients with atypical symptoms. Therefore, developing new diagnostic tools for CAD risk stratification is crucial, as is exploring novel therapeutic targets to enhance and personalize treatment strategies.

In recent years, an increasing number of studies have found a close association between ERS and the development of CAD. The ER stress signaling pathway is frequently activated in myocardial cells and vascular endothelial cells of CAD patients, leading to pathological changes such as abnormal protein folding, endoplasmic reticulum calcium imbalance, and oxidative stress. These changes can promote biological effects such as apoptosis, inflammatory reactions, and vascular remodeling in myocardial cells and vascular endothelial cells, ultimately contributing to the development and progression of CAD. Chronic ER stress can disrupt the secretion function of Paneth and goblet cells, triggering inflammation, cell apoptosis, and mucosal barrier dysfunction.

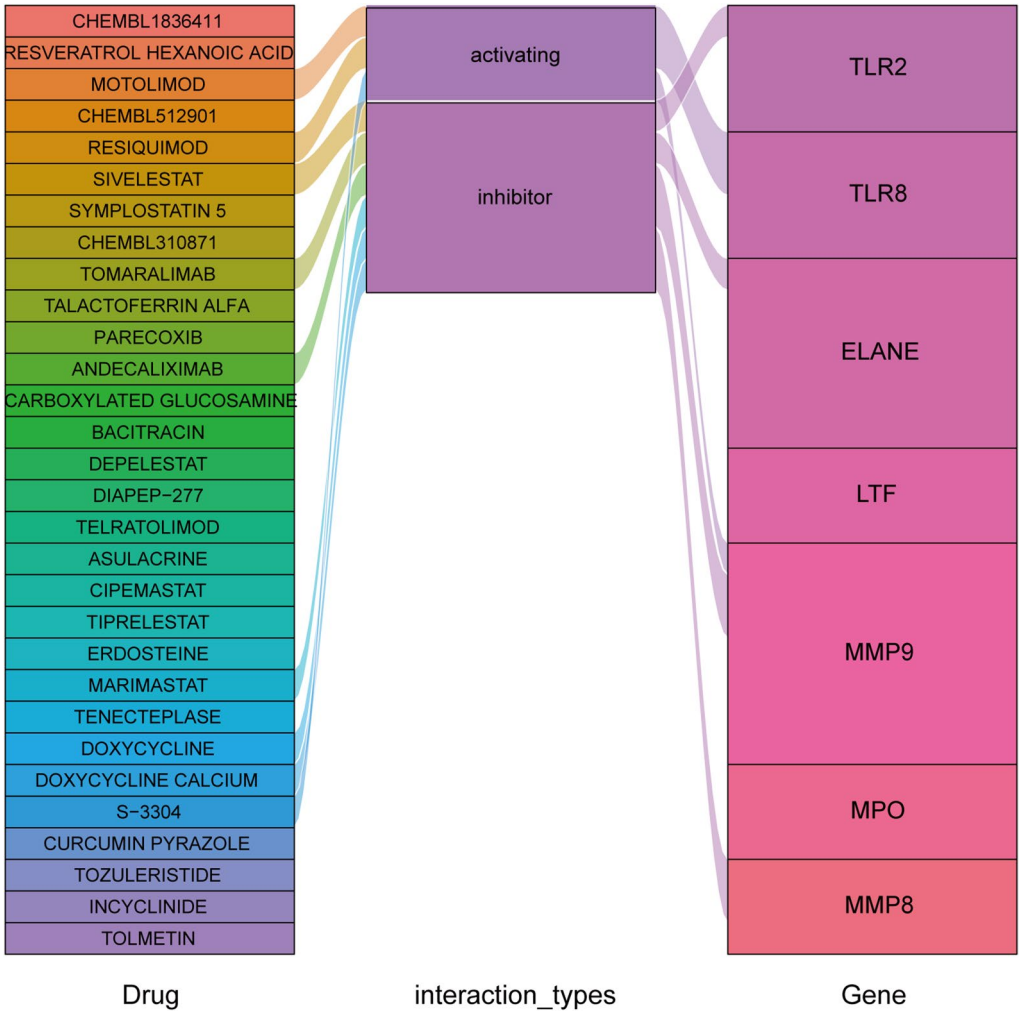

Fig. 10. Drug prediction based on ERSRGs.10 key genes were targeted in the DGIdb database and top 30 potential target drugs/compounds were predicted from the database.

Herb(Pinyin)	TCM ingredients	Target proteins	Enrichment ratio	*P*-value
Ying Xing Ye	3	3	352.15	7.06e-11
Cang Zhu	6	4	52.82	4.86e-09
Su He Xiang	3	3	52.82	1.85e-07
Zhi Gan Cao	3	3	45.60	3.35e-07
Bai Mao Gen	2	3	38.89	6.34e-07
Hu Huang Lian	3	3	37.29	7.50e-07
Ma Gen	1	3	36.85	7.86e-07

Table 3. The BATMAN-TCM database predicts that ERSRGs are most closely associated with Ginkgo Biloba(Ying Xing Ye).

Modulating ER stress may offer new therapeutic strategies for CAD. In this study, we identified ERSRGs using bioinformatics analysis and found notable synergistic interactions among them via correlation analysis.

In this study, we connected ER stress to CAD and explored its potential pathogenic mechanisms, opening new avenues for CAD diagnosis, treatment, and prognosis. We first obtained gene expression data for 16 CAD patients and 14 healthy controls from two GEO datasets, identifying 833 DEGs, of which 507 were upregulated and 326 downregulated. Functional enrichment analysis of these DEGs highlighted significant biological processes, including neutrophil-mediated cytotoxicity and cell killing. Neutrophils are important cells that promote the progression of atherosclerosis. They can increase plaque area and instability by releasing various cytokines and adhesion factors[33], as well as enhance macrophage phagocytosis of lipids and elevate MMP9

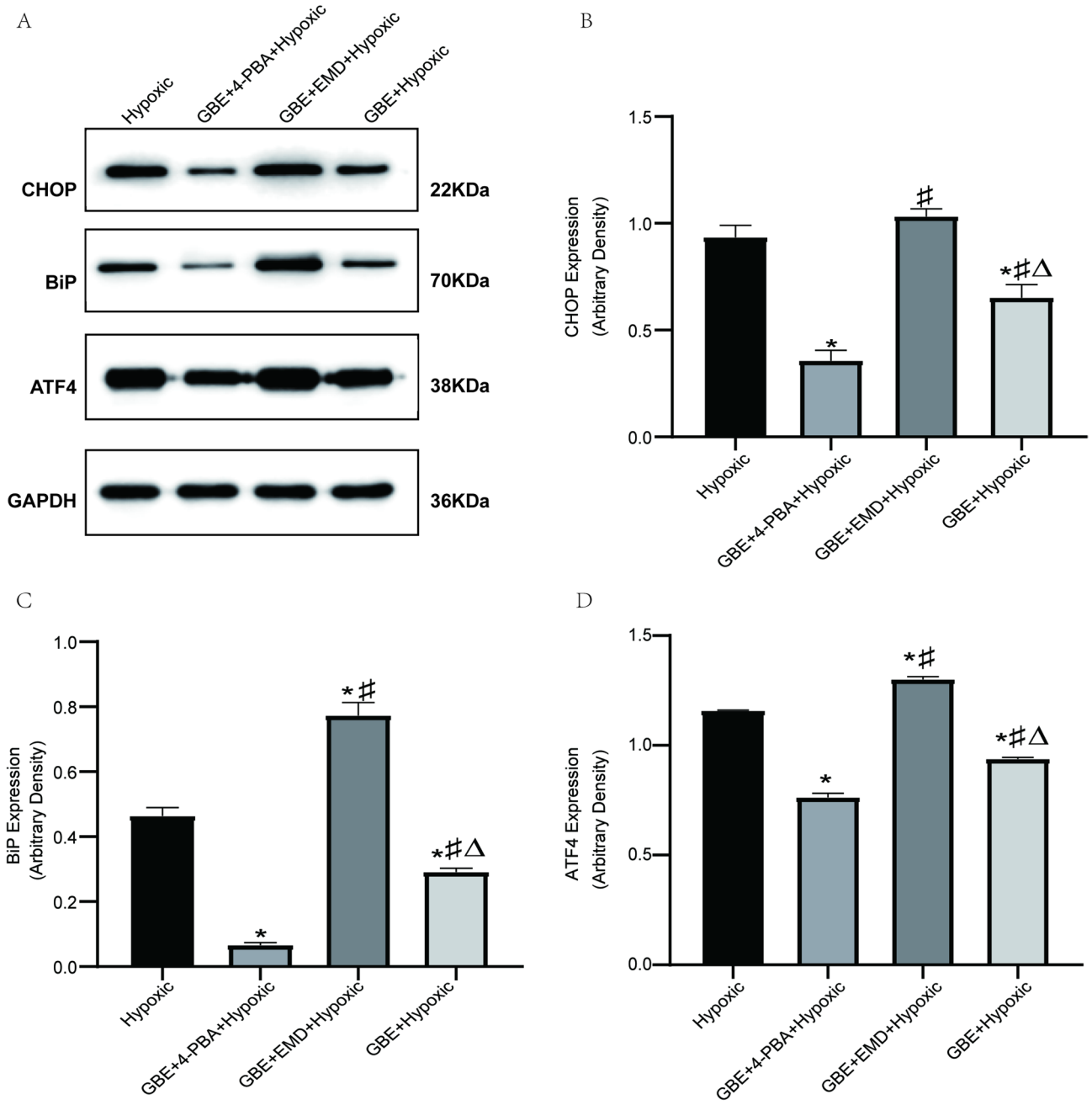

Fig. 11. GBE reversed the activation of ERs. (**A**–**D**)The expression of CHOP, BiP, and ATF4 in H9C2 cardiomyocytes. * represents less than 0.05 compared to the hypoxia group, # represents less than 0.05 compared to the GBE + 4-PBA+hypoxia group, Δ represents less than 0.05 compared to the GBE + EMD+hypoxia group.

levels[34,35]. Previous studies have shown that neutrophil-mediated cytotoxicity and cell killing are characteristic of chronic inflammatory diseases, including CAD, supporting our findings[36,37]. Our results once again confirm the strong association between these two pathways and CAD, suggesting that they deserve continued attention. Therefore, we hypothesize that DEGs play a crucial role in CAD through the regulation of neutrophil-mediated cytotoxicity and cell killing. The cytokines and chemokines released by neutrophils during the inflammatory response can affect the status of surrounding cells, inducing ER stress and thereby altering the processes of protein synthesis and folding. Additionally, reactive oxygen species (ROS) generated during pathogen killing can directly damage intracellular proteins, leading to abnormal folding and triggering the ER stress response. The cytotoxic and cell-killing activities of neutrophils influence ER stress through various mechanisms, subsequently affecting immune responses and cell survival.Additionally, KEGG enrichment analysis indicated that the DEGs are mainly associated with the IL-17 signaling pathway and autophagy. One prominent feature of all inflammatory responses is the infiltration of neutrophils. The recruitment and maintenance of neutrophils

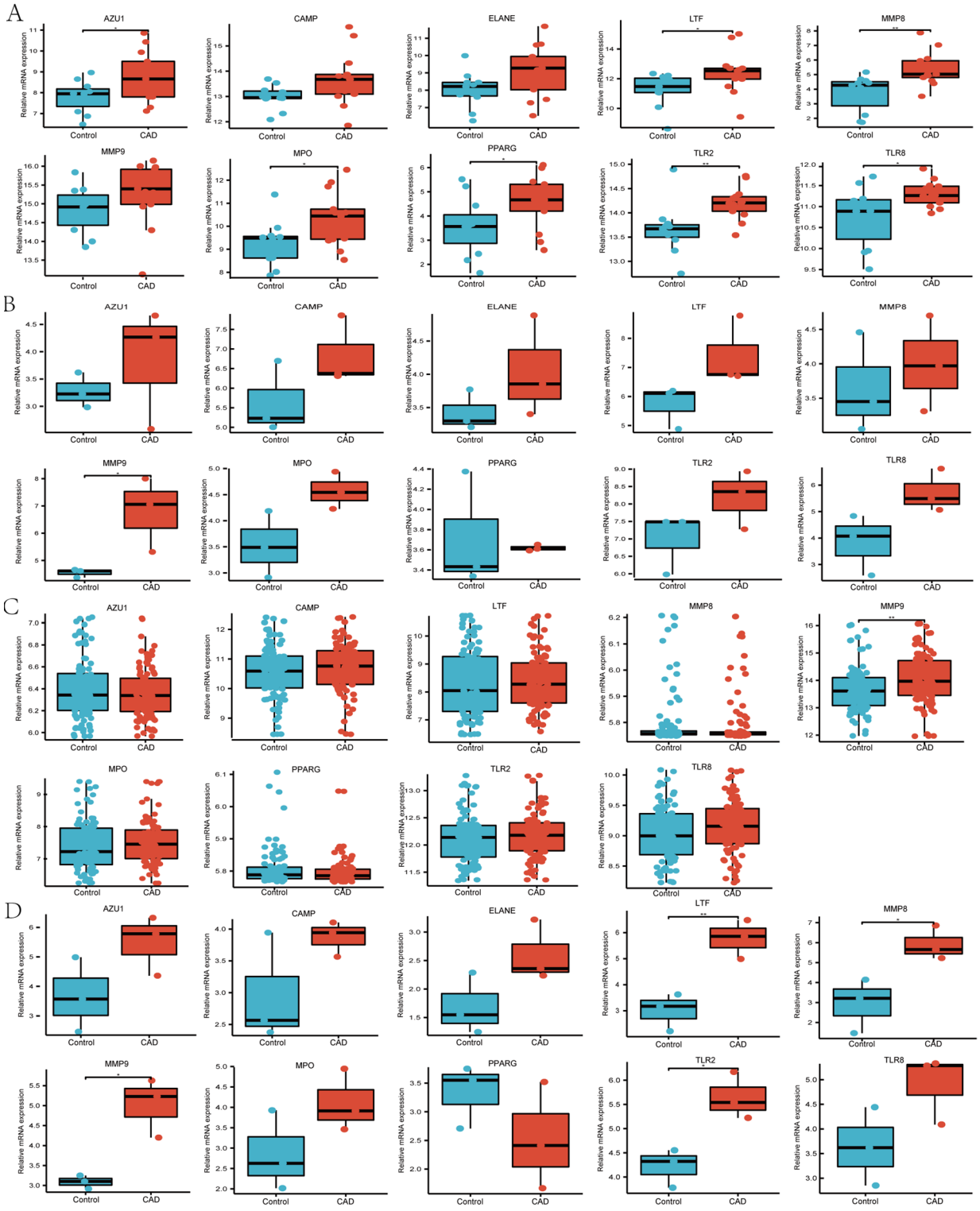

Fig. 12. Single-cell sequencing analysis. (**A**) The UMAP plot shows the unified manifold approximation and projection clustering of 10 clusters from 3 samples. (**B**) Cells from human heart samples were annotated using CellMarker and singleR. (**C**) The violin plot shows the expression levels of hub genes in each cell cluster. (**D**) The localization of ERSRGs in cells of each type. (**E**) The cell proportion plot in the two groups. (F) The hypergeometric test of ERSRGs.

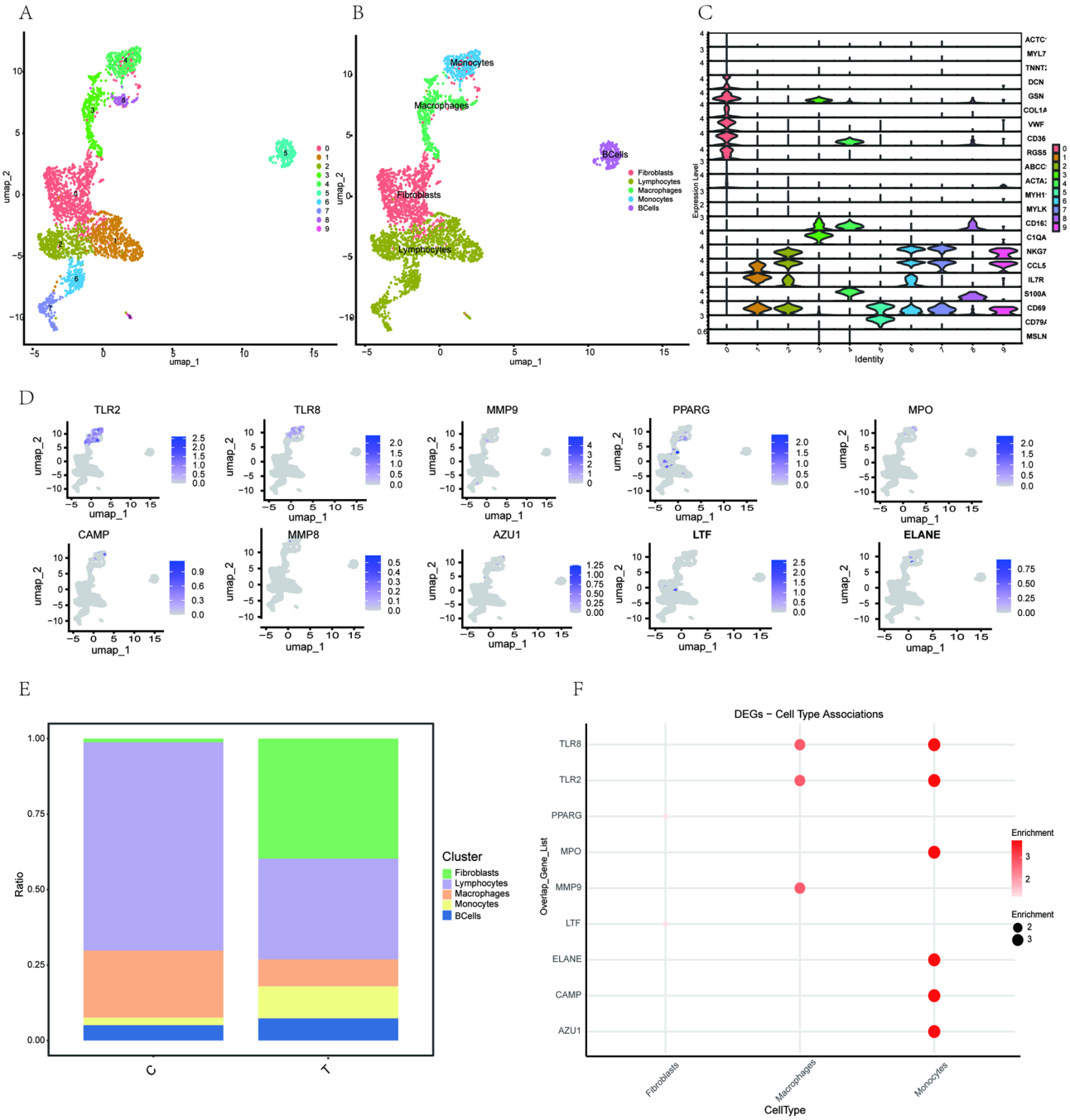

Fig. 13. The expression of the identified top 10 ERSRGs (AZU1, CAMP, ELANE, LTF, MMP8, MMP9, MPO, PPARG, TLR2 and TLR8). The mRNA expression of ERSRGs in GSE42148 (**A**), GSE71226 (**B**) and GSE20681 (**C**). The mRNA expression of ERSRGs from healthy controls and CAD patients as determined by qRT-PCR (**D**). $n = 3$, P-values were shown as: $^{*}P < 0.05$; $^{**}P < 0.01$.

during the inflammatory process involve complex signal transductions, with the IL-17 pathway being the most important.On the other hand, autophagy is a cellular process involved in the degradation and recycling of cellular components, playing a protective role in cellular homeostasis and stress responses. Its role in CAD is associated with its ability to mitigate oxidative stress and inflammation, both of which are key factors in the pathogenesis of atherosclerosis. Dysregulation of autophagy can lead to increased cell death and plaque instability, promoting the progression of CAD[38]. The pro-inflammatory effects of IL-17 may enhance ER stress under inflammatory conditions, and as ER stress intensifies, it may induce the activation of autophagy to remove misfolded proteins and damaged organelles, thereby alleviating cellular damage. The interplay between the IL-17 signaling pathway and autophagy in ER stress is complementary. Therefore, we further hypothesize that the IL-17 signaling pathway and autophagy may be involved in the pathogenesis of CAD by influencing ER stress.

GSEA and GSVA identified key pathways linked to the DEGs, including Hallmark_Unfolded_Protein_Response (UPR). When ER function is impaired, cells activate the UPR to restore normal ER function and ensure proper protein folding and processing. Activation of the UPR promotes autophagy to eliminate misfolded proteins and may induce cell cycle arrest or apoptosis to prevent further damage. Prolonged ER stress can trigger apoptosis in cardiomyocytes, leading to impaired cardiac function and myocardial injury. Additionally, the UPR can facilitate the release of inflammatory factors, exacerbating the progression of atherosclerosis. In the early stages, the UPR may serve as an adaptive response to stress, aiding cardiomyocytes in coping with challenges. However, chronic ER stress can diminish the heart's adaptive capacity, accelerating the progression of CAD[39]. Interventional strategies targeting the UPR and ER stress—such as small molecule drugs and anti-inflammatory therapies—may provide novel approaches for the treatment of CAD.

Using WGCNA for module classification, we identified the bisque4 module ($r = 0.44$, $p = 0.02$) as the key module most strongly correlated with CAD. Using a Venn diagram, we identified 94 genes that were common to ER stress, DEmRNA, and hub genes. Additionally, we used the MCODE plugin in the STRING database to identify two cluster modules, with cluster 1 having a higher score. In total, we identified 10 hub genes, including ELANE, MPO, MMP9, TLR2, TLR8, CAMP, PPARG, LTF, MMP8, and AZU1. We then performed a detailed bioinformatics analysis of the 10 signature genes to explore their gene-gene and gene-disease relationships. Strong positive correlations among these genes suggest their potential synergistic role in CAD development. The AUC values for the 10 genes were all above 0.7, indicating good accuracy and specificity in distinguishing CAD samples from normal ones. Among them, TLR2, TLR8, LTF, and MMP8 ranked in the top four in terms of AUC values.

Our GSEA analysis based on the strictly selected UNFOLDED_PROTEIN_RESPONSE gene set from MSigDB indicates that the UPR pathway is significantly activated in CAD patients (NES = 1.454, FDR = 0.0135). This finding not only confirms the critical role of ER Stress in the pathogenesis of CAD at the pathway level but also provides a reliable biological background for our subsequent analysis of the functions of ERSRGs at the gene level. Furthermore, we quantified the UPR pathway activity for each sample through GSVA and found that the expression of several ERSRGs (such as TLR8, MMP9, etc.) showed a strong positive correlation with UPR activity scores ($r > 0.71$, $p < 0.001$). This result has significant biological implications, indicating that these genes are not merely byproducts of inflammation or immune response but are key molecules that directly participate in or respond to the state of ER Stress. For example, TLR8, as an innate immune receptor, shows a high synchronization of expression with UPR activity, suggesting a previously underappreciated synergistic mechanism between ER Stress and immune activation. More critically, we validated the expression correlation between ERSRGs and core regulatory factors of UPR (such as CHOP/DDIT3, EIF2S1, ERN1, etc.). The significant correlation of genes like TLR2, TLR8, ELANE, AZU1 with these core molecules strongly supports their functional affiliation within the same stress response pathway. In particular, the association of neutrophil-derived proteins such as ELANE and AZU1 with the UPR pathway suggests that different immune cell populations may achieve functional cross-talk through the ER Stress pathway during the progression of CAD. In summary, our analysis delves deeper from the "pathway-gene-molecule" three levels, not only validating the activation state of UPR in CAD but also revealing the functional roles of ERSRGs within it. These findings integrate previously scattered inflammatory markers with the mechanisms of ER Stress, providing a new perspective for understanding the molecular network of CAD and potential biological markers for therapeutic strategies targeting the UPR pathway.

TLR2 is a cell surface receptor that interacts with microbial components such as lipoteichoic acid from gram-positive bacteria, bacterial lipoproteins, and enzymes[40]. TLR2 is present in immune cells, endothelial cells, and epithelial cells. In endothelial cells affected by atherosclerotic plaques, TLR2 expression is significantly elevated and plays a key role in atherosclerosis development[41]. Mullick et al. found that the complete absence of TLR2 in LDL receptor-deficient (LDLR−/−) mice led to reduced atherosclerosis, while TLR2 expression limited to bone marrow-derived cells had no impact on atherosclerosis[42]. The authors showed that treating LDLR−/− mice with Pam3CSK4 (a synthetic TLR2/TLR1 agonist) significantly increased atherosclerotic burden. However, no pro-atherogenic effect was seen in LDLR−/− mice lacking TLR2 or in those with TLR2 deficiency limited to bone marrow-derived cells. This supports the role of TLR2 in promoting atherosclerosis via its action on non-bone marrow-derived cells. MMP8, also known as collagenase-2 or neutrophil collagenase, is associated with inflammatory conditions and is predominantly expressed by neutrophils in atherosclerotic lesions, but also by endothelial cells, smooth muscle cells, and macrophages[43,44]. Endothelial cell apoptosis and release of MMP8 promote the transition from stable to unstable lesions, leading to plaque rupture, with elevated levels of MMP8 found in vulnerable and ruptured plaques[45]. Increased levels of MMP9 in serum have also been shown to be markers of cardiovascular disease[46]. Research on TLR8, LTF, and CAMP is limited, and their connection to CAD remains poorly understood. The biological functions of most signature genes align with previous studies, supporting the reliability of our findings.

cAMP is an important intracellular signaling molecule that regulates various signaling pathways by activating protein kinase A (PKA) and other effector molecules, mainly affecting the development of CAD by regulating coronary artery smooth muscle contraction, endothelial function, and immune response[47]. AZU1 (Azurocidin 1), also known as α-defensin, is a protein primarily found in neutrophils, with antibacterial, immune regulatory, and inflammation response regulatory functions. AZU1 promotes the release of inflammatory factors by activating the NF-KB signaling pathway, thereby driving the formation of atherosclerosis, and can also regulate the migration of neutrophils and other immune cells to the site of inflammation, participating in the inflammatory response related to CAD[48]. TLR8 (Toll-like receptor 8) is a member of the Toll-like receptor family, widely present in immune cells such as dendritic cells, monocytes, macrophages, and endothelial cells, which can exacerbate the progression of CAD through pathways that activate macrophages via the MAPK signaling pathway and induce the secretion of IL-1β and IL-6[49].

The role of immune response in CAD pathogenesis has long been a major focus. Immunity can regulate the body's inflammatory response both directly and indirectly. Immune infiltration also has a dual effect on myocardial cells, with evidence showing it worsens the inflammatory response[50]. Immune cells found in the heart include B cell memory, NK cells, macrophages, monocytes, neutrophils, dendritic cells, T cells, eosinophils, and mast cells, which also play important roles in maintaining cardiac function[51,52]. We used CIBERSORT to assess immune infiltration differences between CAD and normal tissues. The results revealed that immune cell levels were generally higher in CAD patients compared to controls. Notably, B cell memory ($P = 0.048$) and NK cell ($P = 0.013$) infiltration were significantly elevated in CAD patients. B cell is a crucial component of the adaptive immune system, renowned for their roles in antibody production and antigen presentation. Their increased prevalence in patients with CAD suggests an enhanced immune response, which may contribute to inflammation and plaque instability[53]. Similarly, natural killer (NK) cells, as part of the innate immune system, play a pivotal role in targeting and eliminating infected or transformed cells. The heightened infiltration of NK cells in CAD patients may indicate a persistent response to endothelial injury or stress[54]. ER stress can adversely affect the survival of B cells memory through various pathways, including the regulation of antibody synthesis, modulation of apoptosis signals, alteration of cytokine secretion, and changes in cellular metabolism. When the ER encounters stressors such as misfolded proteins or amino acid deprivation, it activates the UPR. The UPR regulates metabolic activities within NK cells by activating specific transcription factors, including XBP1, ATF4, and CHOP, thereby influencing cytokine synthesis and secretion. Furthermore, ER stress affects NK cell function through multiple mechanisms, including the modulation of cytotoxic granule production, alterations in cellular metabolic states, and the dynamics of the immune microenvironment. These interactions underscore the complex relationship between ER stress and immune cell functionality in the context of CAD. We performed a correlation analysis between marker genes and 22 immune cells. The results indicate that immune microenvironment changes in CAD patients may be linked to genes such as MMP9, MMP8, PPARG, MPO, ELEAN, TLR2, and TLR8. In conclusion, our findings, supported by extensive literature, highlight the crucial role of immune cell infiltration in CAD pathogenesis.

The observed increase in B cells and NK cells in CAD patients, along with the correlation with ER stress-related genes, highlights the significance of immune responses in disease progression. This emphasizes the potential therapeutic targets for modulating immune activity in the prevention or treatment of CAD.

Clinically, the diagnosis of most CAD patients is usually made after the onset of angina. Developing genetic-based score models and classifying CAD can enhance clinical diagnosis and treatment accuracy, as well as inform future prevention strategies. In this study, we integrated all three datasets (GSE42148, GSE71226, and GSE20681) and performed an 80/20 split. By identifying the top three DEGs in the expanded training set, we selected TLR2 and MMP9 from the original ten hub genes, which have clear roles in cardiovascular pathophysiology and endogenous stress responses. Ultimately, we identified five robust and biologically reasonable markers: L1TD1, EGR3, CXorf36, TLR2, and MMP9. We established a gene risk scoring model for CAD based on these five genes, which demonstrated certain scoring capabilities. The AUC on the validation set was 0.791, showing better generalization ability and maintaining relatively stable predictive performance. Although the cross-validated AUC on the training set was 0.694, this indicates a better balance between fitting and generalization to some extent, providing a robust predictive framework for the complex pathogenic mechanisms of CAD.

We further examined the regulatory molecular characteristics and potential drug candidates of ERSRGs, mapping the transcription factors and miRNAs associated with each hub gene. Several novel transcription factors, which bind to the promoters of key regulatory genes in differentiated cardiac myocytes, were identified, though they have not been studied previously. Prior research has highlighted the role of transferrin proteins like SRF, GATA-4, HAND2, TBX-20, MEF2C, FOXO, and HEY2 in disease progression[55–57]. We also performed a detailed analysis of the relationship between ERSRGs and the miRNA network. The levels of miR-18a-9p, miR-27a-3p, miR-199a-3p, miR-223-5p, miR-652-3p, and others were found to be closely linked to atherosclerosis and cardiovascular restenosis[58]. The functional role of the predicted gene-targeted drugs remains unclear, and further research is needed to explore specific pathways. Additionally, we obtained results of drug-gene interactions from the DGIdb database. A total of 177 potential drugs or compounds for treating CAD were identified, with most targeting the PPARG gene. The top four drugs with the highest interaction scores targeted the TLR2 and TLR8 genes. Potential drugs for CAMP and AZU1 have not been discovered yet. A deeper understanding of these relationships will facilitate the discovery of gene-targeted drugs and help identify new drug binding sites, providing references for exploring specific ERSRGs as potential therapeutic targets. However, these findings are still in the predictive stage and require further experimental validation.

Through network pharmacology analysis of the BATMAN-TCM database, we found that Ginkgo biloba leaves have a high binding affinity with multiple ERSRGs, suggesting that it may serve as a multi-target formulation to intervene in the UPR pathway. Further in vitro experiments confirmed that GBE treatment significantly downregulated the expression of key ERs markers such as CHOP, BiP and ATF4 in H9c2 cardiomyocytes, indicating that GBE has the ability to alleviate ER stress. Notably, when GBE was used in combination with the ER stress inhibitor 4-PBA, the expression of CHOP, BiP and ATF4 further decreased, demonstrating a synergistic inhibitory effect; however, after co-treatment with GBE and the ER stress inducer tunicamycin (EMD), the expression of CHOP, BiP and ATF4 rebounded. This positive and negative validation strongly suggests that the cardioprotective effect of GBE relies at least partially on its regulation of the ER stress pathway, rather than non-specific effects. These findings provide a molecular-level mechanistic explanation for the traditional application of Ginkgo biloba leaves in cardiovascular diseases and experimental evidence for its new uses. From the perspective of drug action patterns, GBE exhibits characteristics of multi-target and holistic regulation, which highly aligns with the pathological features of CAD as a complex disease involving multiple genes and pathways. The "multi-component-multi-target-multi-pathway" action mode of traditional Chinese medicine formulas, such as GBE, may be particularly suitable for regulating networked stress response systems like UPR. The results

of this study suggest that intervention strategies targeting ER stress do not necessarily require highly selective single-target drugs, and multi-target regulation may be more clinically feasible. In summary, this study not only verifies the positive effect of GBE in alleviating ER stress in cardiomyocytes but also preliminarily reveals that its action depends on the regulation of the UPR pathway. This provides a theoretical basis and experimental support for using GBE as adjunctive therapy for CAD, especially in clinical subtypes with significant ER stress status. Future research could further combine animal models and clinical samples to validate the effects of GBE in regulating ER stress and improving the progression of CAD at an overall level.

This study directly addresses the inherent challenge of cellular heterogeneity in whole blood transcriptome analysis by integrating single-cell RNA sequencing data. Based on scRNA-seq datasets from patients with stable coronary artery disease and acute coronary syndrome, we systematically assessed the distribution characteristics of different cell types in CAD and their contributions to gene expression signals, thereby providing important evidence for elucidating the cellular origins and functional mechanisms of ERSRGs. Clustering analysis identified five major cell types, including fibroblasts, lymphocytes, macrophages, monocytes, and B cells. Notably, the ten ERSRGs we constructed were significantly enriched in monocytes and macrophages, and this spatial distribution characteristic strongly suggests that these genes may participate in the occurrence and development of CAD by regulating the immune modulation, inflammatory response, and immune response processes of monocytes and macrophages. Further analysis revealed that the expression of key genes such as TLR2 and TLR8 was highly restricted to monocytes, while expression in other immune cells was lower, showing a clear cell type specificity. The results of the hypergeometric test further confirmed the significant enrichment of ERSRGs in monocytes (FDR = 0.009, enrichment ratio = 3.7), while no significant enrichment was observed in other cell types such as macrophages and fibroblasts. This monocyte-specific expression pattern not only technically excludes the confounding effects of changes in cell proportions on transcriptome signals but also biologically emphasizes the central role of monocytes in CAD-related ER stress. In the context of disease, monocytes, as the main precursor cells of macrophages in atherosclerotic plaques, have their activation state closely related to the inflammatory level and stability of the plaques. The results of this study indicate that the specific upregulation of ERSRGs in monocytes may reflect the ER stress state of monocytes in the early stages of the disease and the molecular basis for their transition to a pro-inflammatory phenotype. The enrichment of gene expression such as TLR2 and TLR8 further suggests that there is a cross-talk between innate immune signals and ER stress responses in monocytes, which may jointly drive the sustained state of vascular inflammation. In summary, through single-cell level analysis, we not only validated the cell type specificity of ERSRGs in transcriptome changes but also provided cellular context evidence for their functional mechanisms in CAD. These findings reinforce the role of monocytes as key effector cells in ER stress and provide theoretical support for the future development of cell type-targeted intervention strategies.

The RT-qPCR results from peripheral blood samples of CAD patients in our clinical study were largely consistent with our data analysis findings. However, there are several limitations in our research. First, since all data were obtained from a single database, there may be potential selection bias. Additionally, we lacked detailed clinical information, such as age, gender, smoking history, and family history, which could influence gene expression. We used patient blood samples for experimental validation of gene expression with a limited sample size. Although the results are consistent with our bioinformatics predictions and show statistical significance for several key genes, larger and prospective cohort studies are needed in the future to fully establish the clinical utility of these biomarkers. Finally, the data in this study comes from Indian and Chinese populations, and factors such as genetic background, environmental exposure, and lifestyle vary among populations, which may affect the association between genes and diseases. Therefore, the results of this study should be applied cautiously to other populations (such as European and American populations). Future research should be conducted in multiple population cohorts to validate and assess the potential impact of population heterogeneity on the results, and further enhance the general applicability of the research conclusions.

Conclusion

In summary, we used a series of bioinformatics analyses to ultimately identify and validate 10 ERSRGs (*MMP9*, *TLR2*, *TLR8*, *CAMP*, *LTF*, *MMP8*, *PPARG*, *MPO*, *ELANE*, *AZU1*) in CAD.The CAD gene risk score model formed by the 5 genes L1TD1, EGR3, CXorf36, TLR2, and MMP9 has a certain discriminative ability for the risk of CAD.Our study also identified 177 potential drugs/compounds for treating CAD based on the ERSRGs identified and predicted a strong effect of GBE in regulating ER stress. Single-cell analysis further strengthened the reliability of the study. Looking ahead, these findings provide a foundation for future experimental validation and clinical trials aimed at elucidating the role of these genetic factors in CAD and developing targeted therapeutic strategies. This study highlights the potential of bioinformatics in advancing our understanding of complex diseases and underscores the necessity of continued interdisciplinary approaches to translate these insights into clinical practice.

Data availability

Publicly available datasets were analyzed in this study. This data can be found here: https://www.ncbi.nlm.nih.gov/geo/. The accession numbers are GSE20681, GSE71226, GSE42148, GSE184073 and GSE180678.

Received: 12 March 2025; Accepted: 12 March 2026
Published online: 22 March 2026

References

1. Roth, G. A. et al. Global burden of cardiovascular diseases and risk factors, 1990–2019: Update from the GBD 2019 study. *J. Am. Coll. Cardiol.* **76**(25), 2982–3021 (2020).
2. Klarin, D. & Natarajan, P. Clinical utility of polygenic risk scores for coronary artery disease. *Nat. Rev. Cardiol.* **19**(5), 291–301 (2022).
3. Kim, H. J. et al. Inhibition of endoplasmic reticulum stress alleviates lipopolysaccharide-induced lung inflammation through modulation of NF-κB/HIF-1α signaling pathway. *Sci. Rep.* **3**, 1142 (2013).
4. Haas, M. J. et al. Transcription factor EB protects against endoplasmic reticulum stress in human coronary artery endothelial cells. *Eur. J. Pharmacol.* **933**, 175274 (2022).
5. Mooradian, A. D. & Haas, M. J. Cardioprotective antihyperglycemic drugs ameliorate endoplasmic reticulum stress. *Am. J. Physiol. Cell. Physiol.* **326**(1), C89–c94 (2024).
6. Haas, M. J. et al. Differential effects of cyclooxygenase-2 (COX-2) inhibitors on endoplasmic reticulum (ER) stress in human coronary artery endothelial cells. *Vascul Pharmacol.* **142**, 106948 (2022).
7. Lee, A. S. GRP78 induction in cancer: Therapeutic and prognostic implications. *Cancer Res.* **67**(8), 3496–3499 (2007).
8. Harding, H. P., Zhang, Y. & Ron, D. Protein translation and folding are coupled by an endoplasmic-reticulum-resident kinase. *Nature* **397**(6716), 271–274 (1999).
9. Langfelder, P. & Horvath, S. WGCNA: an R package for weighted correlation network analysis. *BMC Bioinform.* **9**, 559 (2008).
10. Szklarczyk, D. et al. STRING v11: protein-protein association networks with increased coverage, supporting functional discovery in genome-wide experimental datasets. *Nucleic Acids Res.* **47**(D1), D607–d13 (2019).
11. Barrett, T. et al. NCBI GEO: archive for functional genomics data sets–update. *Nucleic Acids Res.* **41**(Database issue), D991–D995 (2013).
12. Edgar, R., Domrachev, M. & Lash, A. E. Gene Expression Omnibus: NCBI gene expression and hybridization array data repository. *Nucleic Acids Res.* **30**(1), 207–210 (2002).
13. Irizarry, R. A. et al. Exploration, normalization, and summaries of high density oligonucleotide array probe level data. *Biostatistics* **4**(2), 249–264 (2003).
14. Ritchie, M. E. et al. limma powers differential expression analyses for RNA-sequencing and microarray studies. *Nucleic Acids Res.* **43**(7), e47 (2015).
15. Kanehisa, M. et al. KEGG: biological systems database as a model of the real world. *Nucleic Acids Res.* **53**(D1), D672–d7 (2025).
16. Kanehisa, M. Toward understanding the origin and evolution of cellular organisms. *Protein Sci.* **28**(11), 1947–1951 (2019).
17. Kanehisa, M. & Goto, S. KEGG: kyoto encyclopedia of genes and genomes. *Nucleic Acids Res.* **28**(1), 27–30 (2000).
18. Yu, G., Wang, L. G., Han, Y. & He, Q. Y. clusterProfiler: an R package for comparing biological themes among gene clusters. *Omics* **16**(5), 284–287 (2012).
19. Subramanian, A. et al. Gene set enrichment analysis: a knowledge-based approach for interpreting genome-wide expression profiles. *Proc. Natl. Acad. Sci. U S A.* **102**(43), 15545–15550 (2005).
20. Gustavsson, E. K. et al. ggtranscript: an R package for the visualization and interpretation of transcript isoforms using ggplot2. *Bioinformatics* **38**(15), 3844–3846 (2022).
21. Hänzelmann, S., Castelo, R. & Guinney, J. GSVA: gene set variation analysis for microarray and RNA-seq data. *BMC Bioinform.* **14**, 7 (2013).
22. Szklarczyk, D. et al. The STRING database in 2021: customizable protein-protein networks, and functional characterization of user-uploaded gene/measurement sets. *Nucleic Acids Res.* **49**(D1), D605–d12 (2021).
23. Shannon, P. et al. Cytoscape: a software environment for integrated models of biomolecular interaction networks. *Genome Res.* **13**(11), 2498–2504 (2003).
24. Chen, B. et al. Profiling tumor infiltrating immune cells with CIBERSORT. *Methods Mol. Biol.* **1711**, 243–259 (2018).
25. Zhang, S. et al. Immune infiltration in renal cell carcinoma. *Cancer Sci.* **110**(5), 1564–1572 (2019).
26. Han, H. et al. TRRUST v2: an expanded reference database of human and mouse transcriptional regulatory interactions. *Nucleic Acids Res.* **46**(D1), D380–d6 (2018).
27. Dweep, H., Gretz, N. & Sticht, C. miRWalk database for miRNA-target interactions. *Methods Mol. Biol.* **1182**, 289–305 (2014).
28. Chen, Y. & Wang, X. miRDB: an online database for prediction of functional microRNA targets. *Nucleic Acids Res.* **48**(D1), D127–d31 (2020).
29. Cotto, K. C. et al. DGIdb 3.0: a redesign and expansion of the drug-gene interaction database. *Nucleic Acids Res.* **46**(D1), D1068–d73 (2018).
30. Sun, K., Li, Y. Y. & Jin, J. A double-edged sword of immuno-microenvironment in cardiac homeostasis and injury repair. *Signal. Transduct. Target. Ther.* **6**(1), 79 (2021).
31. Schrottmaier, W. C., Mussbacher, M., Salzmann, M. & Assinger, A. Platelet-leukocyte interplay during vascular disease. *Atherosclerosis* **307**, 109–120 (2020).
32. Bobryshev, Y. V. Dendritic cells and their role in atherogenesis. *Lab. Invest.* **90**(7), 970–984 (2010).
33. Zhao, T. et al. Antigen-presenting cell-like neutrophils foster T Cell response in hyperlipidemic patients and atherosclerotic mice. *Front. Immunol.* **13**, 851713 (2022).
34. Moniot, A. et al. Inhibition of recruitment and activation of neutrophils by pyridazinone-scaffold-based compounds. *Int. J. Mol. Sci.*, **23**(13). (2022).
35. Conforti, A., Wahlers, T. & Paunel-Görgülü, A. Neutrophil extracellular traps modulate inflammatory markers and uptake of oxidized LDL by human and murine macrophages. *PLoS One.* **16**(11), e0259894 (2021).
36. Döring, Y., Soehnlein, O. & Weber, C. Neutrophil extracellular traps in atherosclerosis and atherothrombosis. *Circ. Res.* **120**(4), 736–743 (2017).
37. Buso, G. et al. The role of neutrophils in lower limb peripheral artery disease: State of the art and future perspectives. *Int. J. Mol. Sci.* **24**(2). (2023).
38. Zhou, M., Dai, W., Cui, Y. & Li, Y. Estrogen downregulates gp130 expression in HUVECs by regulating ADAM10 and ADAM17 via the estrogen receptor. *Biochem. Biophys. Res. Commun.* **523**(3), 753–758 (2020).
39. Mozzini, C., Cominacini, L., Garbin, U. & Fratta Pasini, A. M. Endoplasmic reticulum stress, NRF2 signalling and cardiovascular diseases in a nutshell. *Curr. Atheroscler Rep.* **19**(8), 33 (2017).
40. Zähringer, U. et al. TLR2 - promiscuous or specific? A critical re-evaluation of a receptor expressing apparent broad specificity. *Immunobiology* **213**(3-4), 205–224 (2008).
41. Edfeldt, K., Swedenborg, J., Hansson, G. K. & Yan, Z. Q. Expression of toll-like receptors in human atherosclerotic lesions: a possible pathway for plaque activation. *Circulation* **105**(10), 1158–1161 (2002).
42. Mullick, A. E., Tobias, P. S. & Curtiss, L. K. Modulation of atherosclerosis in mice by Toll-like receptor 2. *J. Clin. Invest.* **115**(11), 3149–3156 (2005).
43. Sorsa, T. et al. Matrix metalloproteinases: contribution to pathogenesis, diagnosis and treatment of periodontal inflammation. *Ann. Med.* **38**(5), 306–321 (2006).
44. Lenglet, S., Mach, F. & Montecucco, F. Role of matrix metalloproteinase-8 in atherosclerosis. *Mediators Inflamm.* **2013**, 659282. (2013).
45. Naruko, T. et al. Neutrophil infiltration of culprit lesions in acute coronary syndromes. *Circulation* **106**(23), 2894–2900 (2002).

46. Yabluchanskiy, A. et al. Matrix metalloproteinase-9: Many shades of function in cardiovascular disease. *Physiol. (Bethesda)*. **28**(6), 391–403 (2013).
47. Ebert, A. et al. Proteasome-dependent regulation of distinct metabolic states during long-term culture of human iPSC-derived cardiomyocytes. *Circ. Res.* **125**(1), 90–103 (2019).
48. Zhang, N. et al. Neutrophil degranulation and myocardial infarction. *Cell. Commun. Signal.* **20**(1), 50 (2022).
49. Gao, Y. et al. YAP/TEAD1 complex is a default repressor of cardiac toll-like receptor genes. *Int. J. Mol. Sci.* **22**(13). (2021).
50. Yang, L. et al. MicroRNA-21 prevents excessive inflammation and cardiac dysfunction after myocardial infarction through targeting KBTBD7. *Cell. Death Dis.* **9**(7), 769 (2018).
51. Pattarabanjird, T. et al. Chemokine receptor activation enhances memory B cell class switching linked to IgE sensitization to alpha gal and cardiovascular disease. *Front. Cardiovasc. Med.* **8**, 791028 (2021).
52. Kumrić, M., Kurir, T. T., Borovac, J. A. & Božić, J. The role of natural killer (NK) cells in acute coronary syndrome: A comprehensive review. *Biomolecules*. **10**(11). (2020).
53. Ishizaka, N. IgG4-related disease underlying the pathogenesis of coronary artery disease. *Clin. Chim. Acta*. **415**, 220–225 (2013).
54. Kuijpers, T. W. et al. Longstanding obliterative panarteritis in Kawasaki disease: lack of cyclosporin A effect. *Pediatrics* **112**(4), 986–992 (2003).
55. Giri, P., Mukhopadhyay, A., Gupta, M. & Mohapatra, B. Dilated cardiomyopathy: a new insight into the rare but common cause of heart failure. *Heart Fail. Rev.* **27**(2), 431–454 (2022).
56. Sveinbjornsson, G. et al. Variants in NKX2-5 and FLNC cause dilated cardiomyopathy and sudden cardiac death. *Circ. Genom Precis Med.* **11**(8), e002151 (2018).
57. Mittal, A. et al. Role of cardiac TBX20 in dilated cardiomyopathy. *Mol. Cell. Biochem.* **414**(1-2), 129–136 (2016).
58. Vegter, E. L. et al. Low circulating microRNA levels in heart failure patients are associated with atherosclerotic disease and cardiovascular-related rehospitalizations. *Clin. Res. Cardiol.* **106**(8), 598–609 (2017).

Acknowledgements

We are very grateful to the GEO database for providing meaningful datasets.

Author contributions

LY conceptualized the study, drafted the initial manuscript, and participated in all stages of experimental design, data acquisition, and analysis. FW contributed to data organization and experimental oversight, assisting in manuscript preparation and revisions. FZ and CQ provided critical input on study design, data review, and intellectual content, and was responsible for final manuscript approval. All authors participated in the revision of the manuscript, and read and approved the final manuscript.

Funding

This work was supported by grants from Guangzhou Health Science and Technology General Guidance Program(20261A011101), Science and Technology Projects in Guangzhou (2023A03J0422) and Guangdong Provincial Department of Education (2023KTSCX107),Guangzhou Major Medical Disciplines Project(2025–2027).

Declarations

Ethics statement

This study involving humans was approved by the First Affiliated Hospital of Bengbu Medical College Clinical Medical Research Ethics Committee. All of the experimental procedures involving patients were conducted in accordance with the Clinical Medical Research Ethics Committee of the First Affiliated Hospital of Bengbu Medical College, China.

Competing interests

The authors declare no competing interests.

Additional information

Supplementary Information The online version contains supplementary material available at https://doi.org/10.1038/s41598-026-44541-1.

Correspondence and requests for materials should be addressed to F.-j.Z., C.Q. or L.-l.Y.